



Aalto University
School of Engineering



Development of novel GPR prototypes for the evaluation of asphalt properties

*Prof. Terhi Pellinen, PhD student Ari Hartikainen
Department of Civil Engineering*

*Prof. Pekka Eskelinen
Department of Electrical Engineering and Automation*

**COST Action TU1208 “Civil engineering applications of Ground Penetrating Radar”
25-27.9.2017, Final Conference of the Action
National Institute of Telecommunications of Poland, Warsaw, Poland**

Outline

RVE for asphalt

Types of radars developed in Finland

Field Tests

Calibration of radars







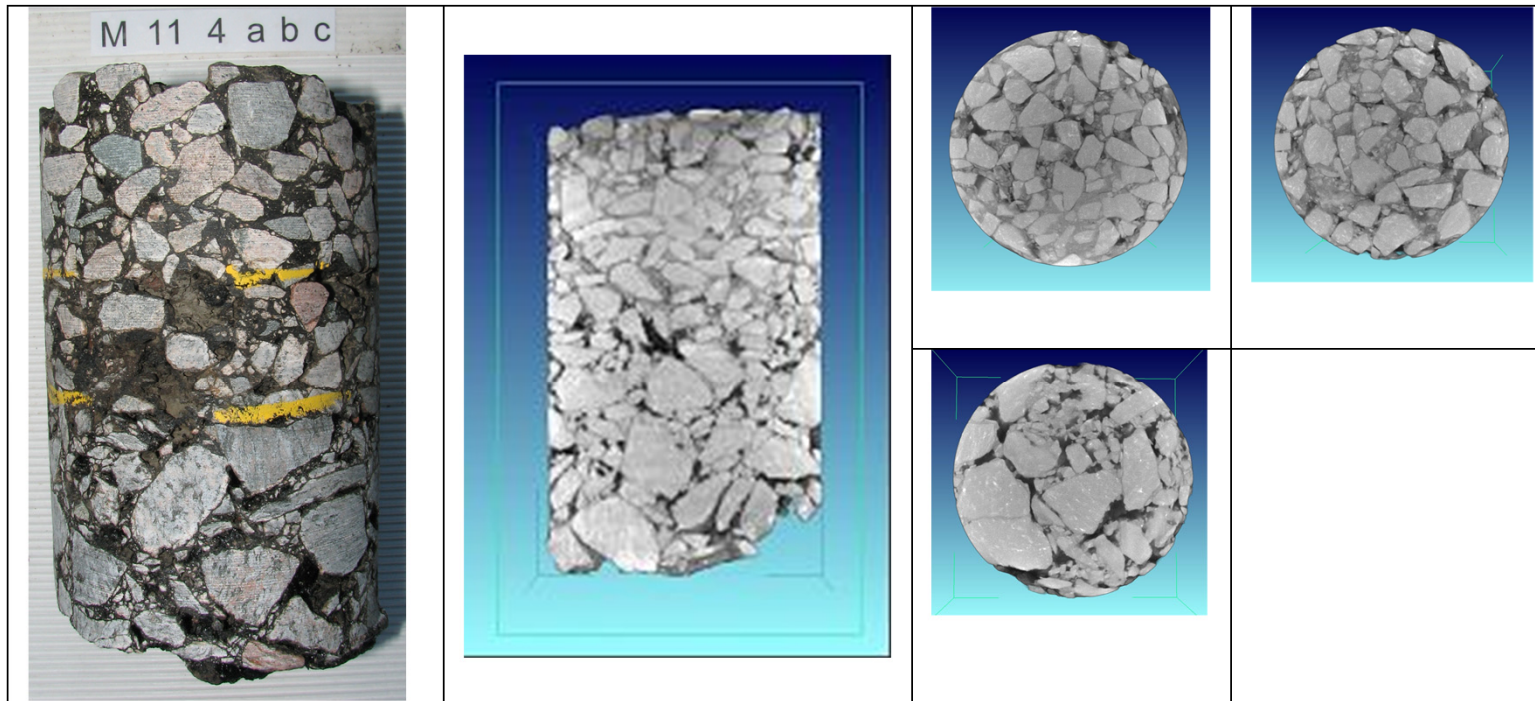








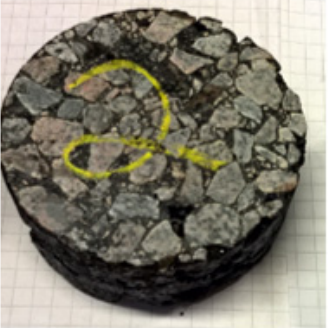
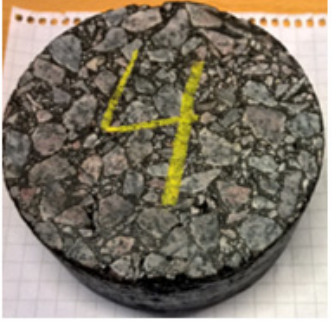

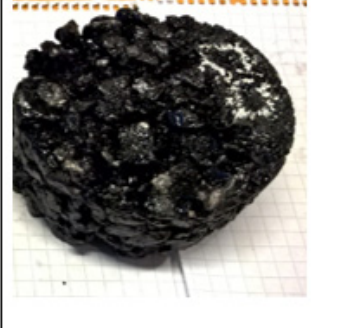




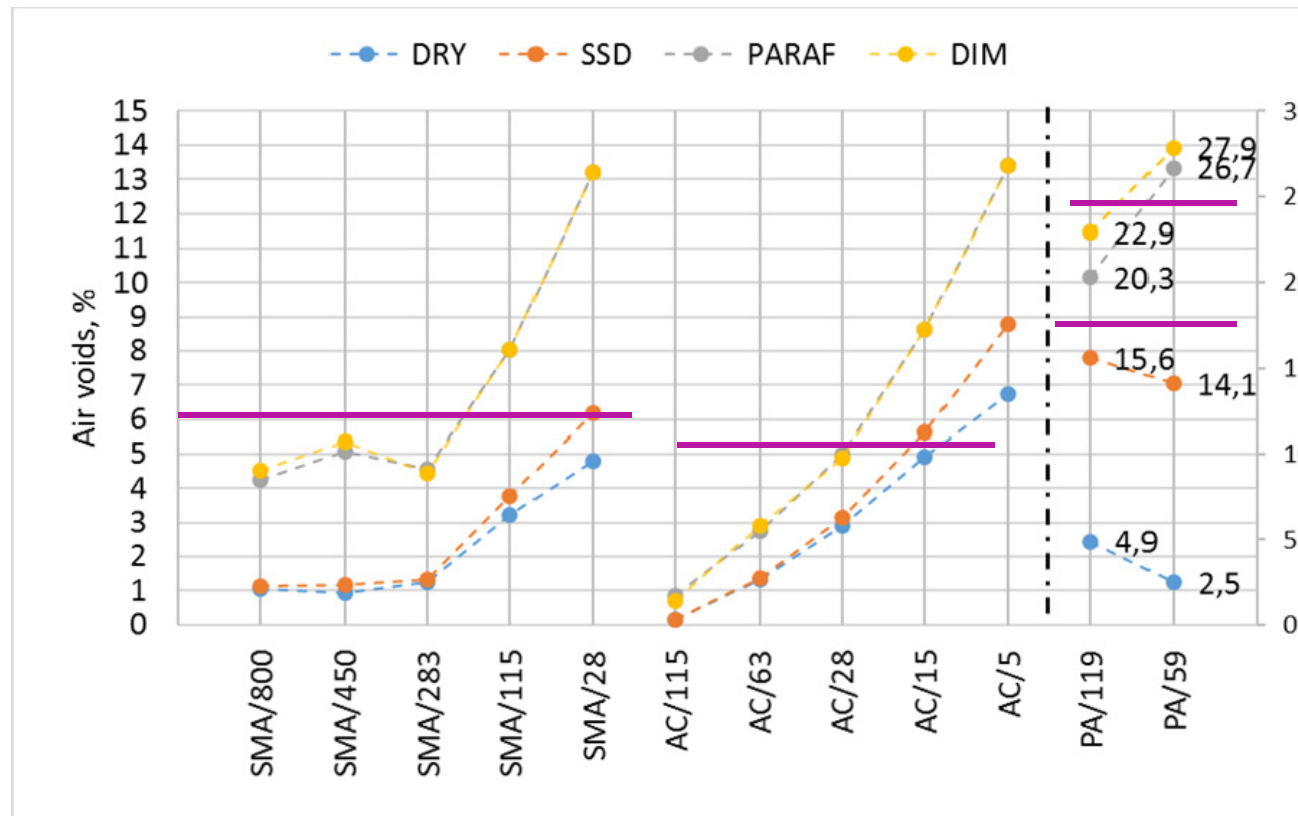
X-Ray scans of asphalt



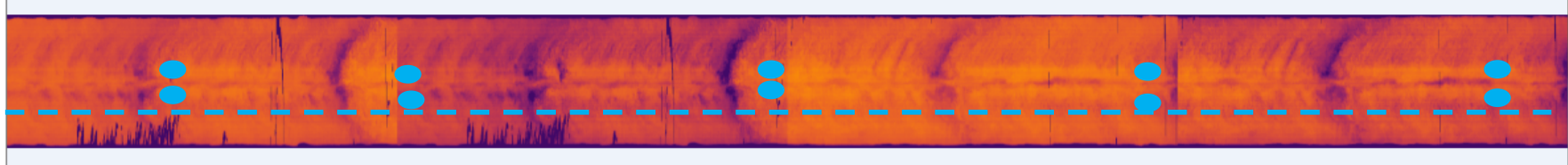
Lab Compaction Trial

			
SMA/800, $V_{SSD} = 1,1\%$	AC/115, $V_{DRY} = 0,2\%$	AC/5, $V_{DRY} = 6,7\%$	PA/119, $V_{DIM} = 22,9\%$
			
SMA/450, $V_{SSD} = 1,2\%$	AC/115, $V_{DRY} = 0,2\%$	AC/15, $V_{DRY} = 4,9\%$	PA/59, $V_{DIM} = 27,9\%$

Gyratory compacted specimens

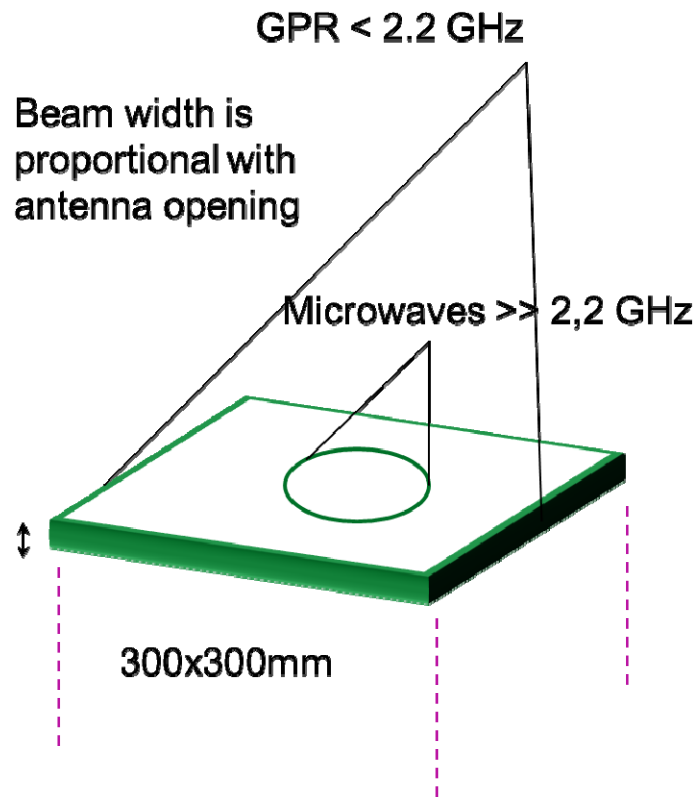


Asphalt inhomogeneity



- **Common study scheme is to take physical core samples from the road and measure the air void content in the laboratory**
 - Expensive, slow
 - Independent samples → Statistical QC/QA
- **Non-destructive (GPR) methods are faster and have a greater spatial coverage longitudinally**
 - Cheap, fast
 - Point accuracy is less than with the laboratory measurements
 - Autocorrelation

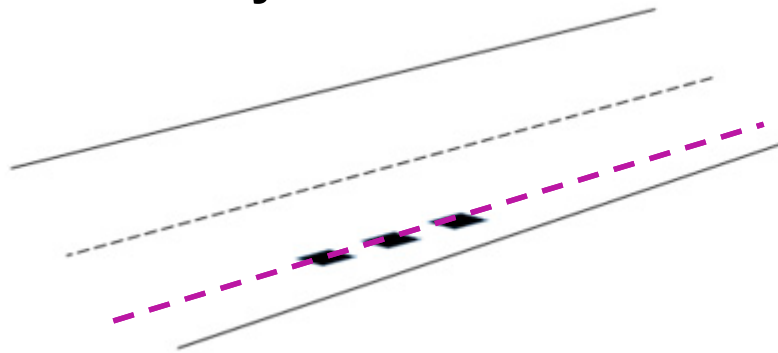
Beam width, antenna footprint



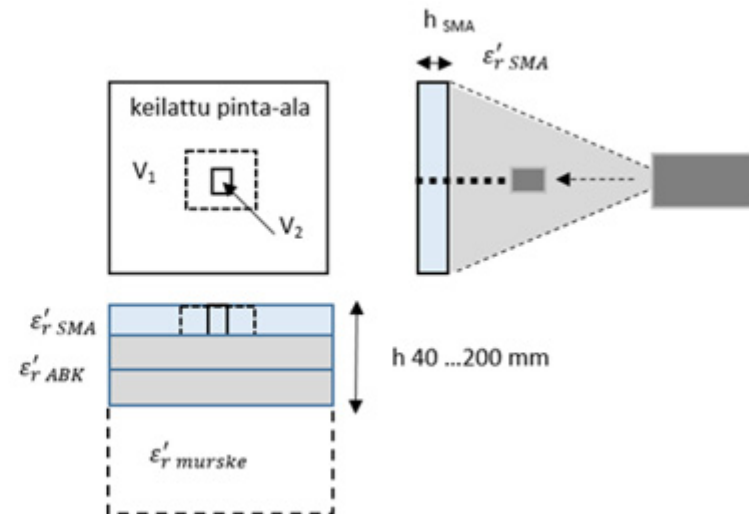
- The wavelength of the microwave signal must be much shorter than the sample thickness in order to be able to distinguish between multiple reflections.
- As a bonus we get very good spatial resolution along the surface.
- For example, the granularity of asphalt can be seen at frequencies above 10 GHz.

Representative Volume Element (RVE)

Assessment of thin (30 - 50 mm) surface layer

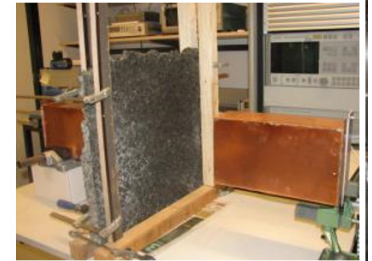


Transmission through sample

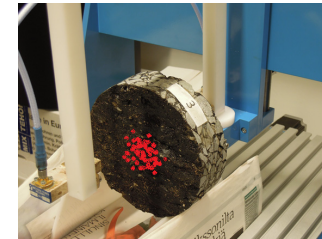
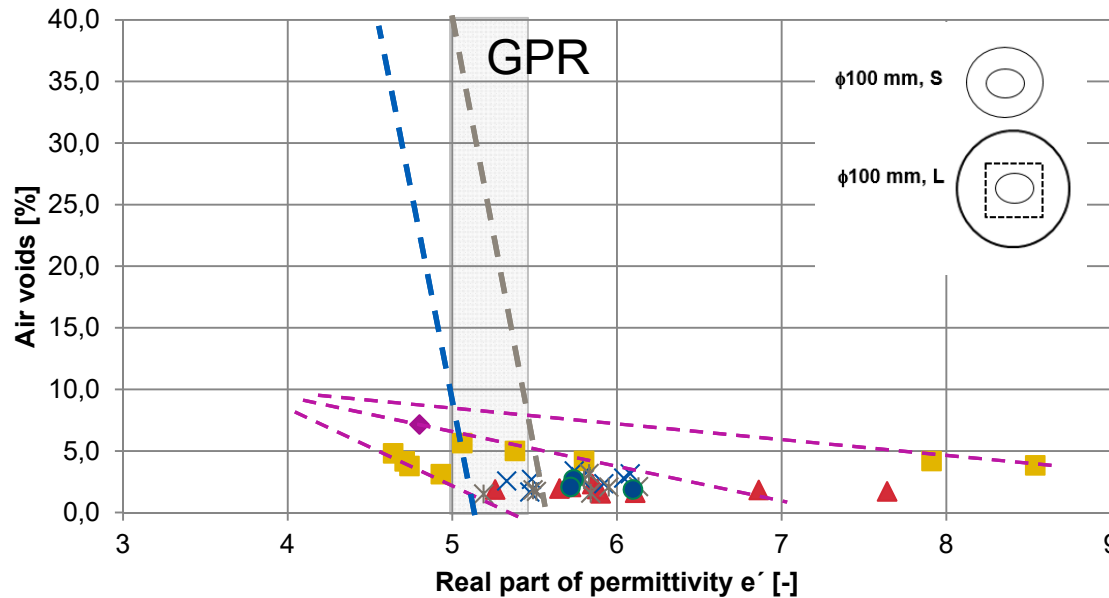


Pellinen T., Huuskonen-Snicker E. and Eskelinen P. 2015a. Representative volume element of asphalt pavement for electromagnetic measurements, *Journal of Traffic and Transportation Engineering (English Edition)*, Special Issue: Functional Pavement Materials and Characterization, Volume 2, Issue 1, Pages 30–39.

Transmission through sample Lab VNA measurements



Permittivity measured 2014 with VNA

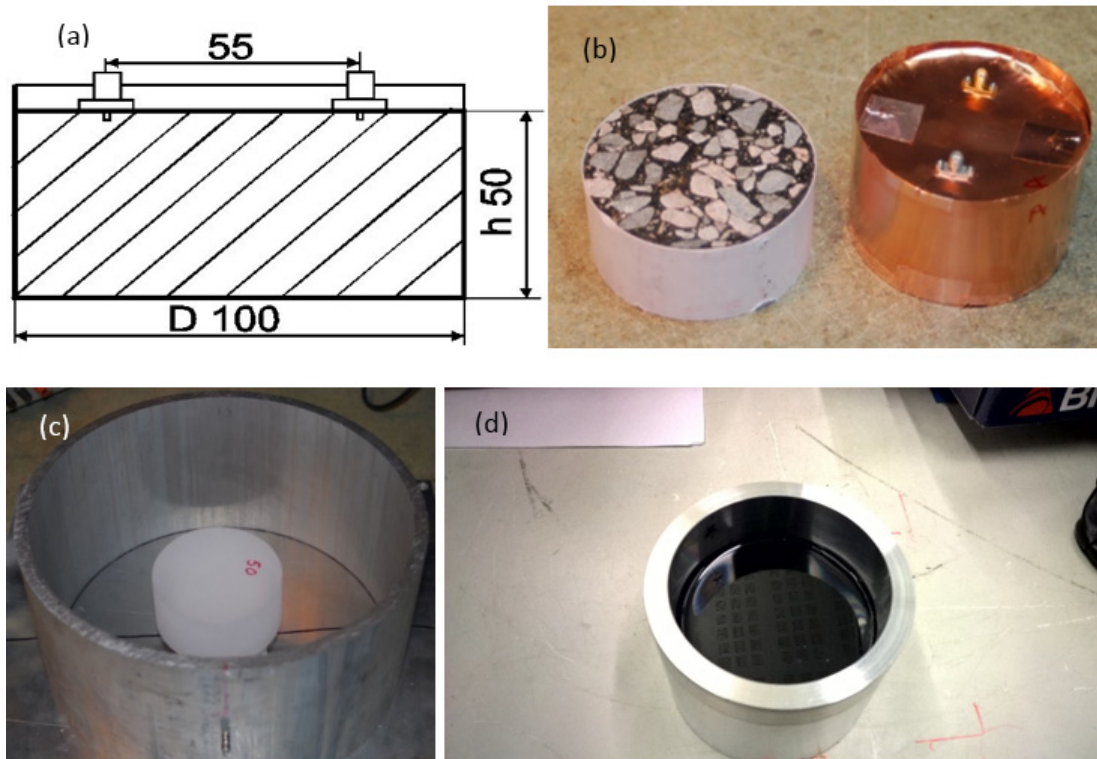


- S samples
- ◆ Slab
- ▲ L samples 1-9
- × L samples 10-18
- ✱ L samples 20-27
- Average L1-9, L10-18, L20-27

$$\sqrt{\epsilon_{eff}} = \sum_i \sqrt{\epsilon_i} V_i$$

Cavity resonator

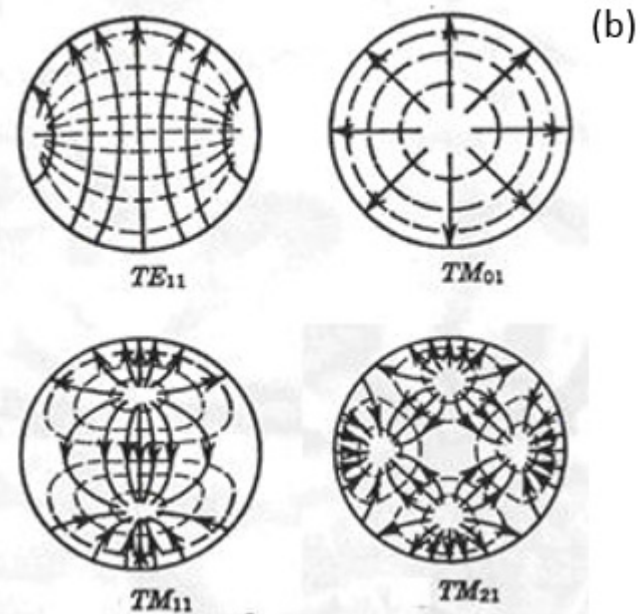
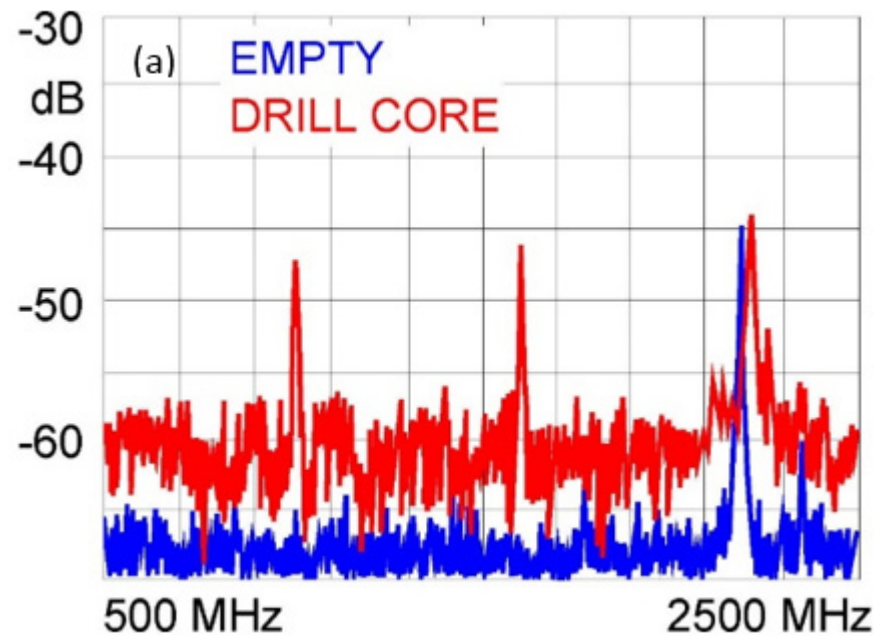
Eskelinen, P. (2016). A Simple Permittivity Calibration Method for GPR-Based Road Pavement Measurements. *Frequenz*, Vol 70, Issue 9-10 (Sep 2016).



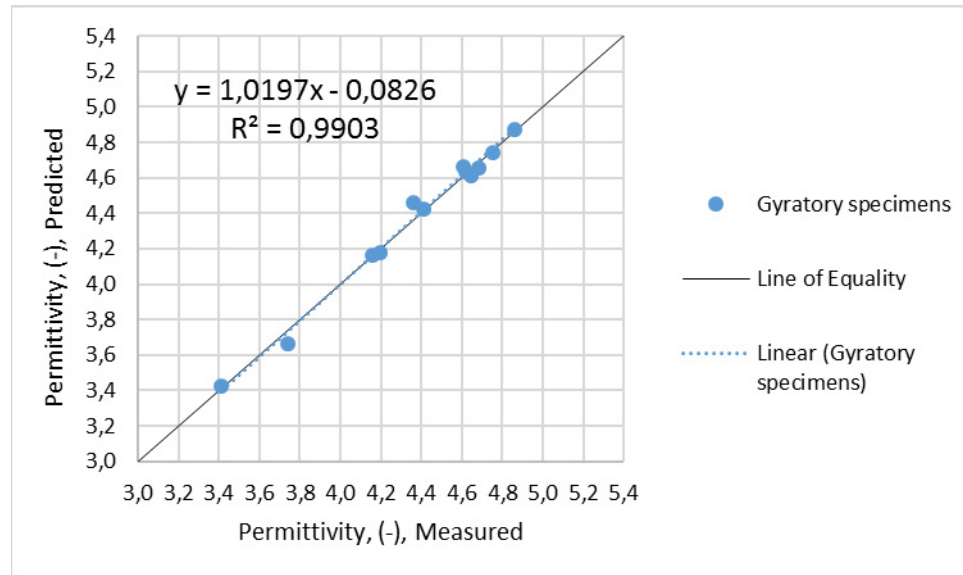
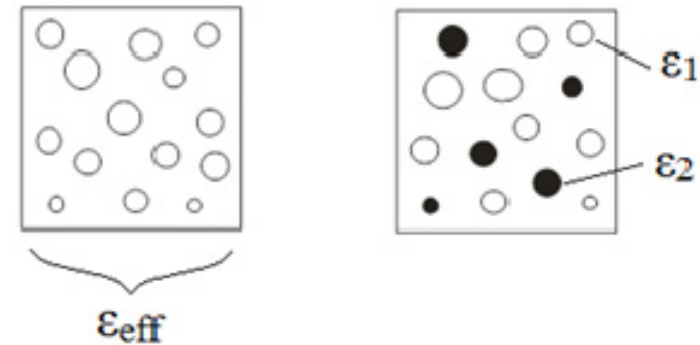
Measurements 1-2 GHz frequency.

For CR method repeatability is 0.02 units of permittivity, when measuring the same sample repeatedly.

EM Transverse modes in CR



Modelling



$$\epsilon'_{r,eff} = \left[\sum V_i (\epsilon'_{r,i})^\alpha \right]^{\frac{1}{\alpha}}$$

With the correlation coefficient R^2 of 0.99, the data fitting gave α a value of **0.375**.

TM_{010} α was **0,48**



Aalto University
School of Engineering

Types of radars

Own radar configurations

- a) a continuous-wave frequency sweeping (FMCW) 1-2 GHz system, partly similar to Zych (2011),
- b) a 12-18 GHz FM device described in detail in Huuskonen-Snicker et al. (2015)
- c) a 32 GHz fixed frequency system.

Both the 1-2 GHz and 12-18 GHz devices utilize inverse FFT to get the time domain reflection response of the pavement surface.

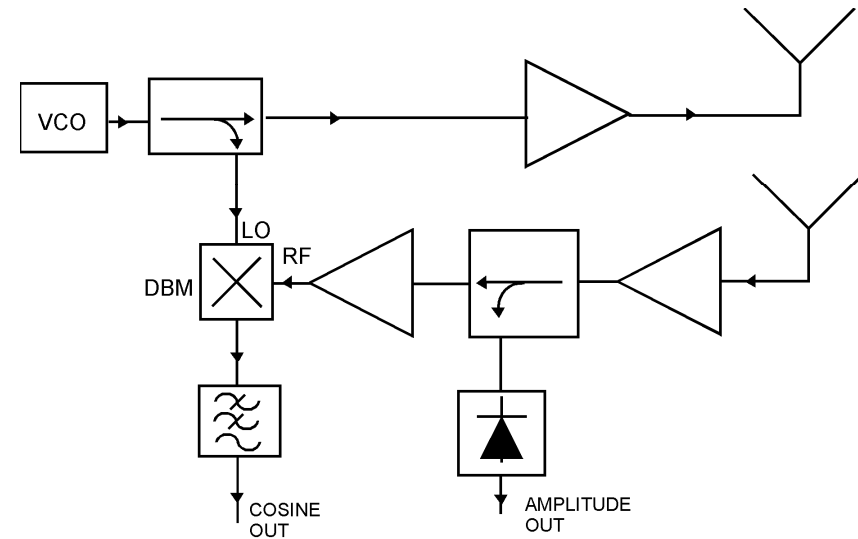
After this, basic reflection coefficient calculus (Ramo and Whinnery 1960) is applied to get the air-asphalt interface permittivity at the correct time window, the location of which is now automated from the raw IFFT plot.

12-18 GHz

Huuskonen-Snicker, Eeva; Eskelinen, Pekka; Pellinen, Terhi; Olkkonen, Martta-Kaisa, (2015) A New Microwave Asphalt Radar Rover for Thin Surface Civil Engineering Applications, *FREQUENZ*, Vol 69, Issue 7-8 (2015).



Figure 4. Ready asphalt radar rover on the street. The two monopole antennas are for vehicle telecommand and for radar telemetry. Radar antennas point towards the road in the front of the car.



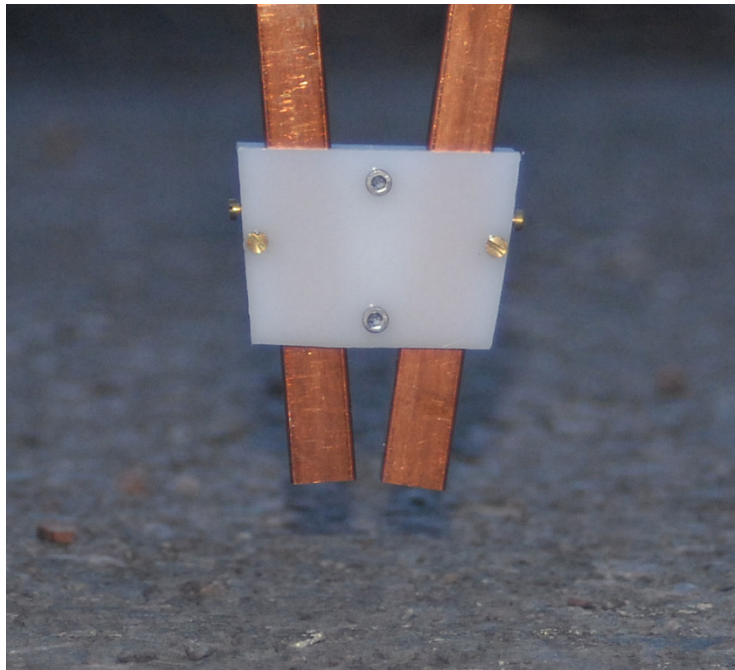
Radar unit block diagram. Amplitude information is obtained from an envelope detector. The cosine of the phase angle comes by the low pass filtering the DBM output.

12-18 GHz

Table 1. *Radar characteristics*

Frequency range	12-18 GHz
Transmitter power	> +10 dBm
Receiver noise figure	< 3dB
Receiver 1 dB compression point	0 dBm
Sweep time	< 12 ms (depends on communication port)
A/D resolution	10 bits
Antennas	2 x 2 dBi
Polarization	linear

Example of antenna focusing arrangement, here applied at 32 GHz.





Aalto University
School of Engineering

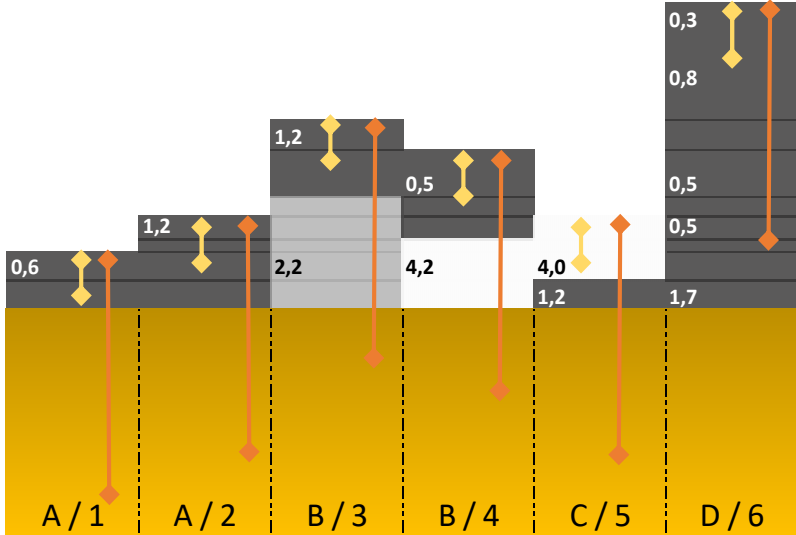
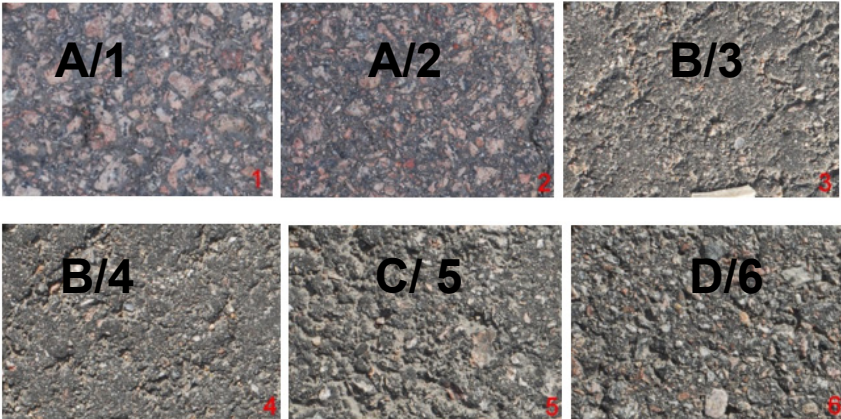
Field Tests



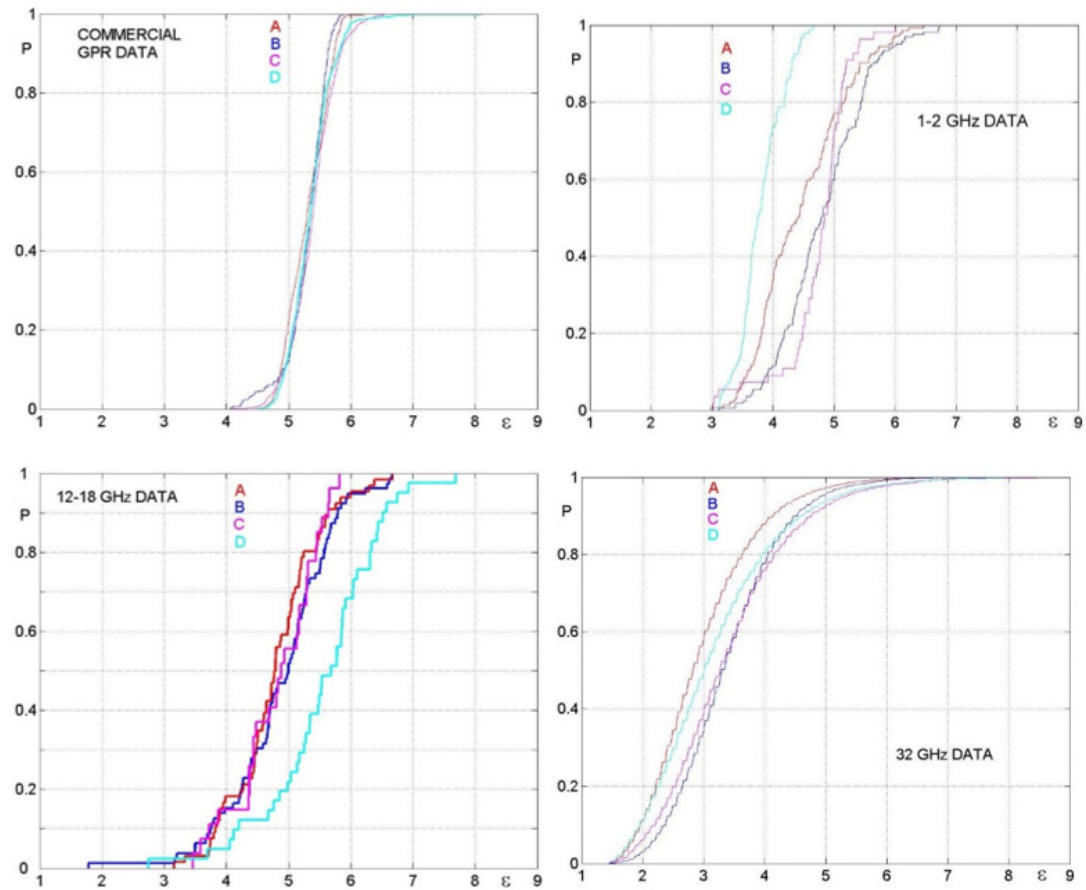
Field trial of 4 radars

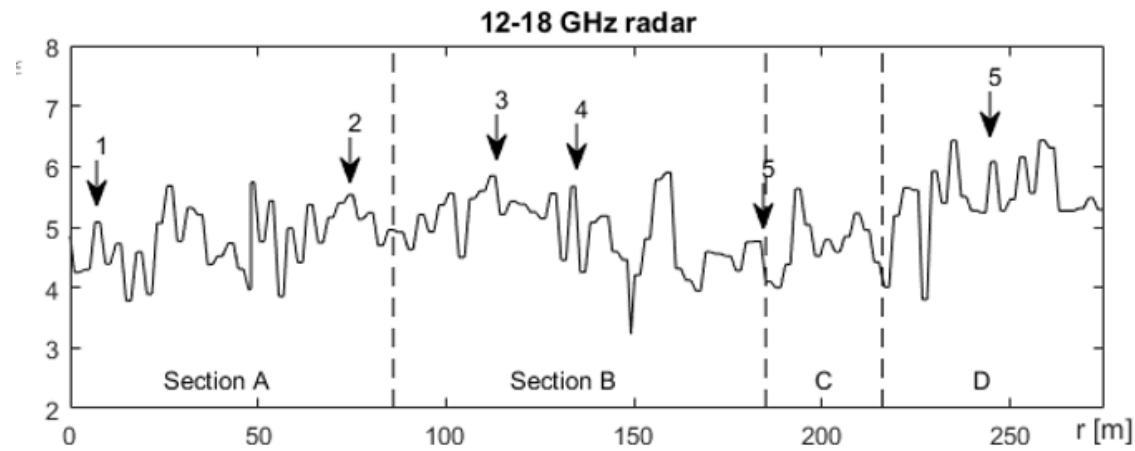
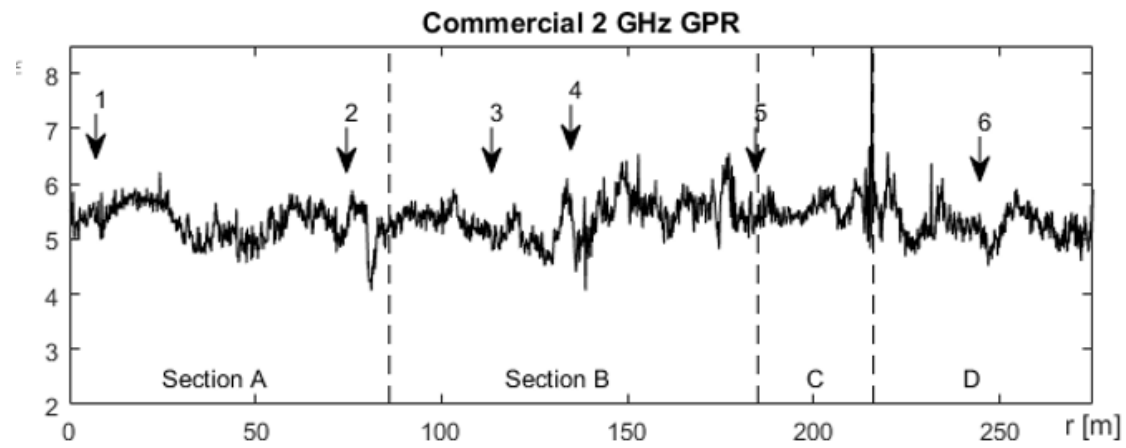
- Standard commercial 2 GHz GPR data, obtained with SIR-30 system from GSSI Inc (USA) was selected as reference for the remaining three devices.
- Main GPR parameters were as follows: measurement time 20 ns, sweep count 1024 samples, sweep rate 500 scans/s, data width 32 bits.
- Test road 250 m, 4 different pavement sections.

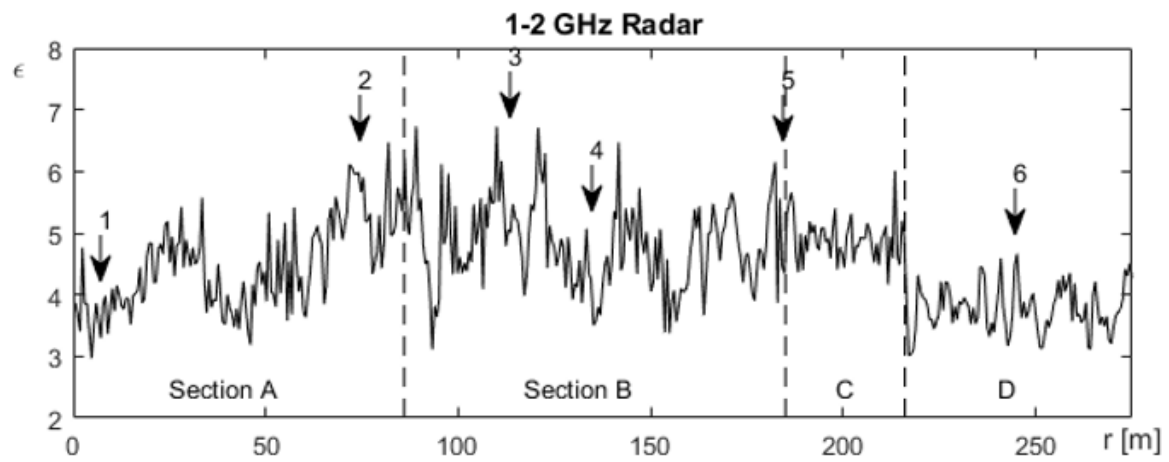
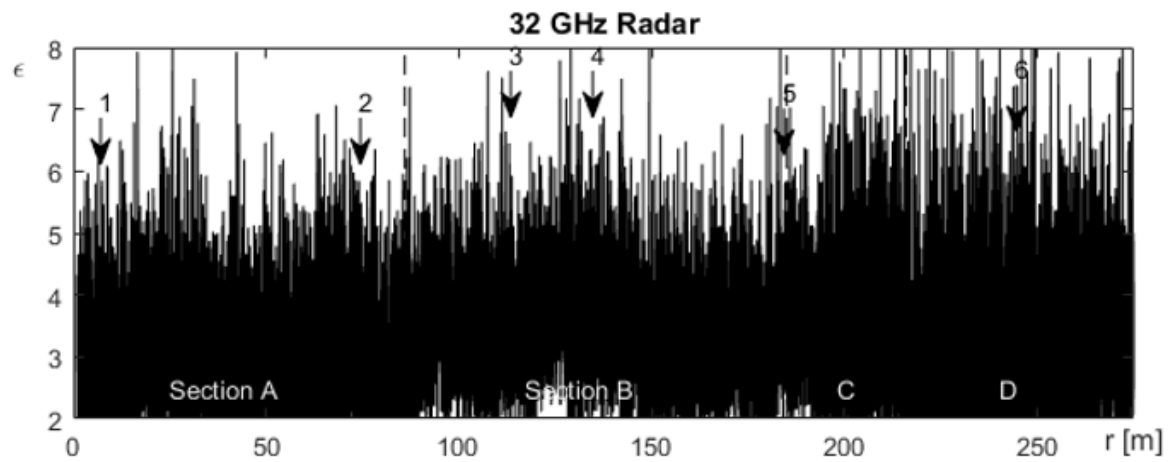
Test Road, variable AC thickness

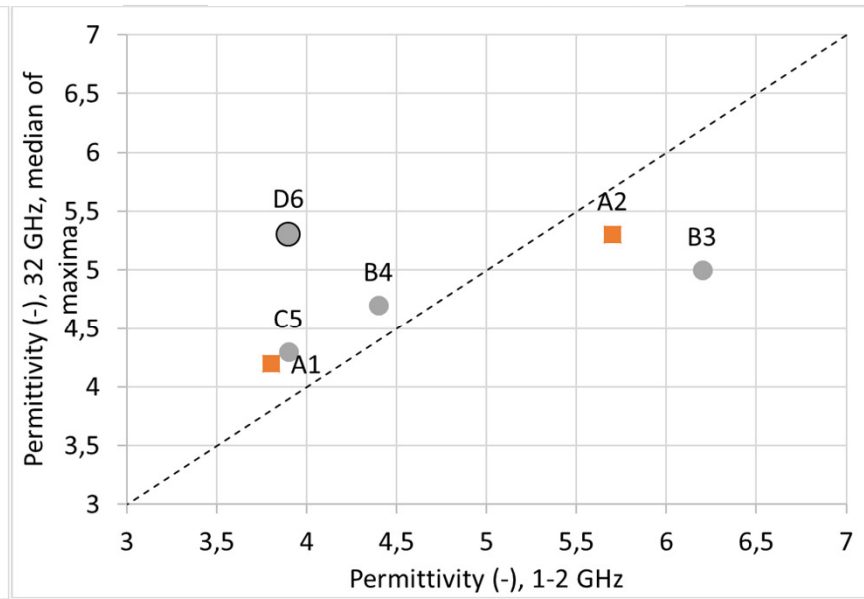
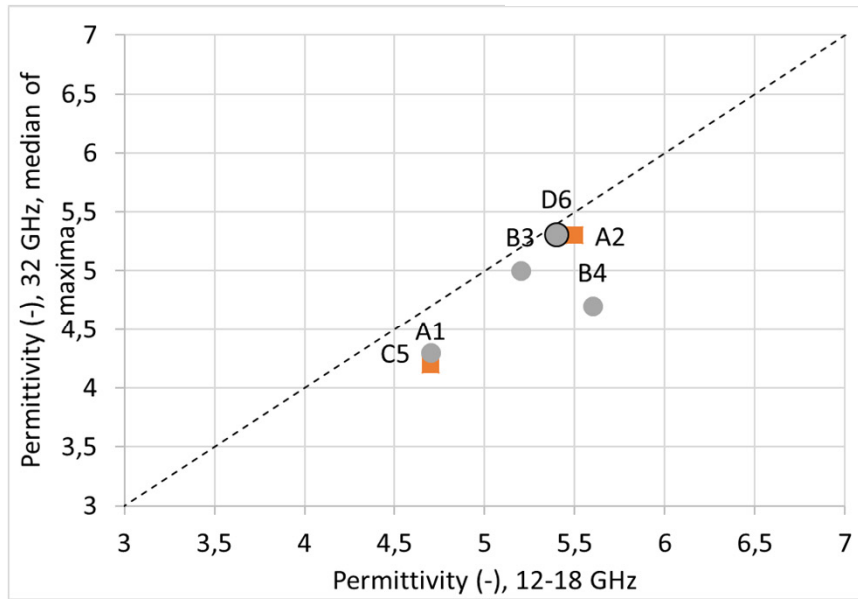
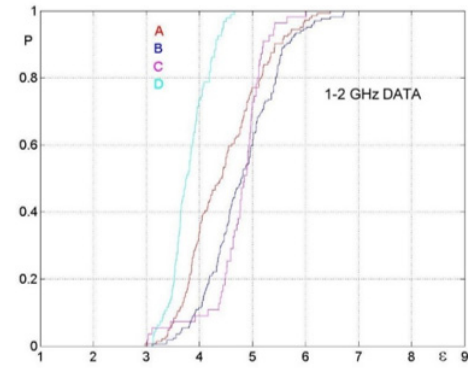
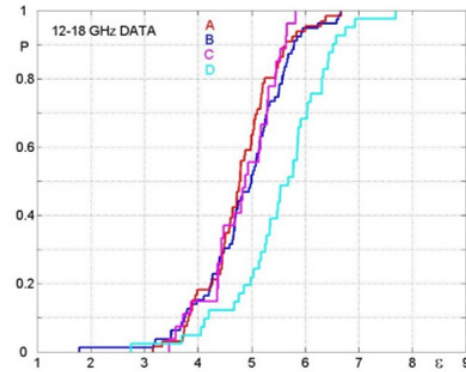
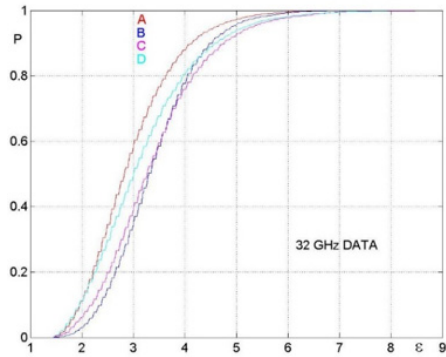


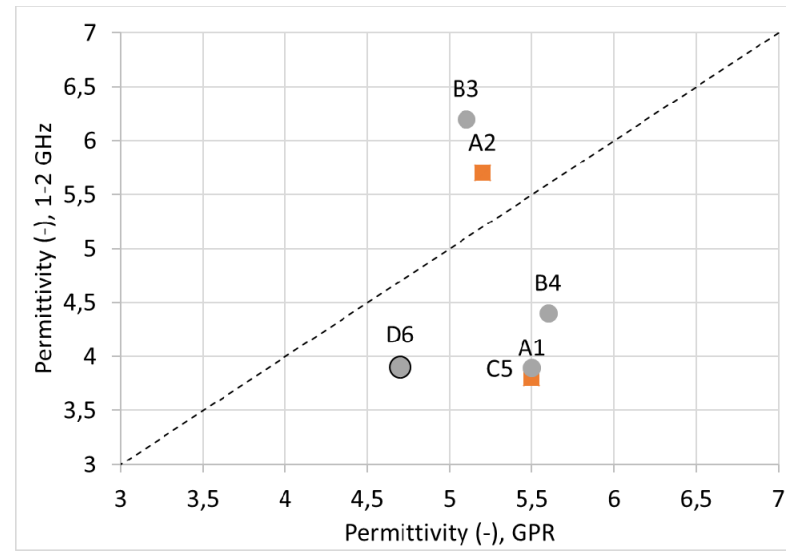
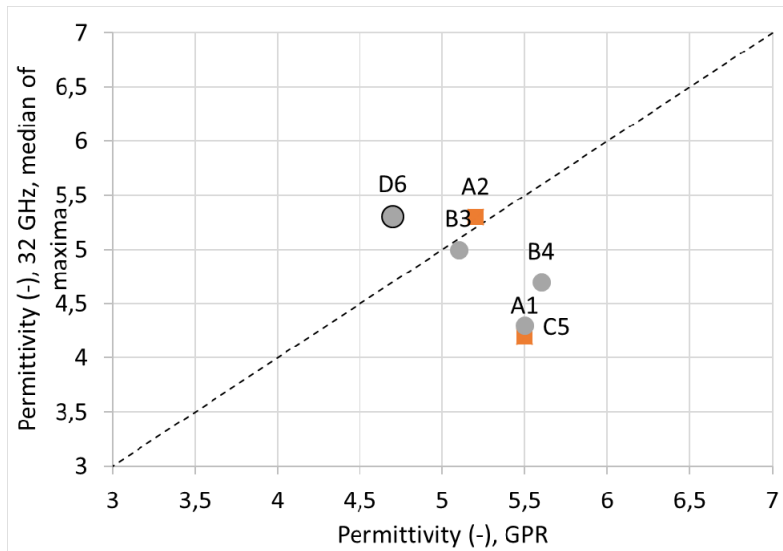
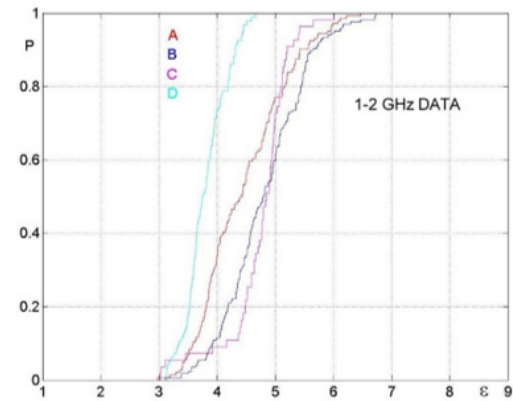
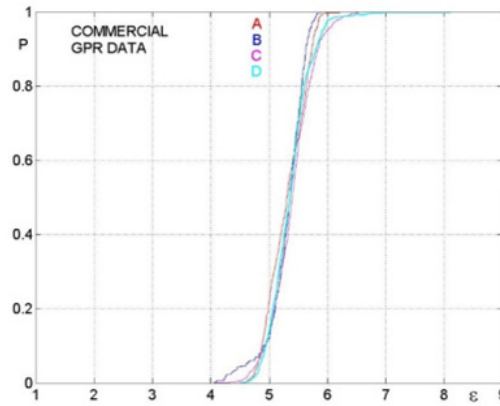
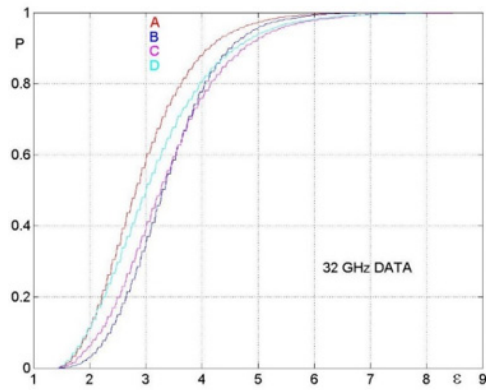
Results







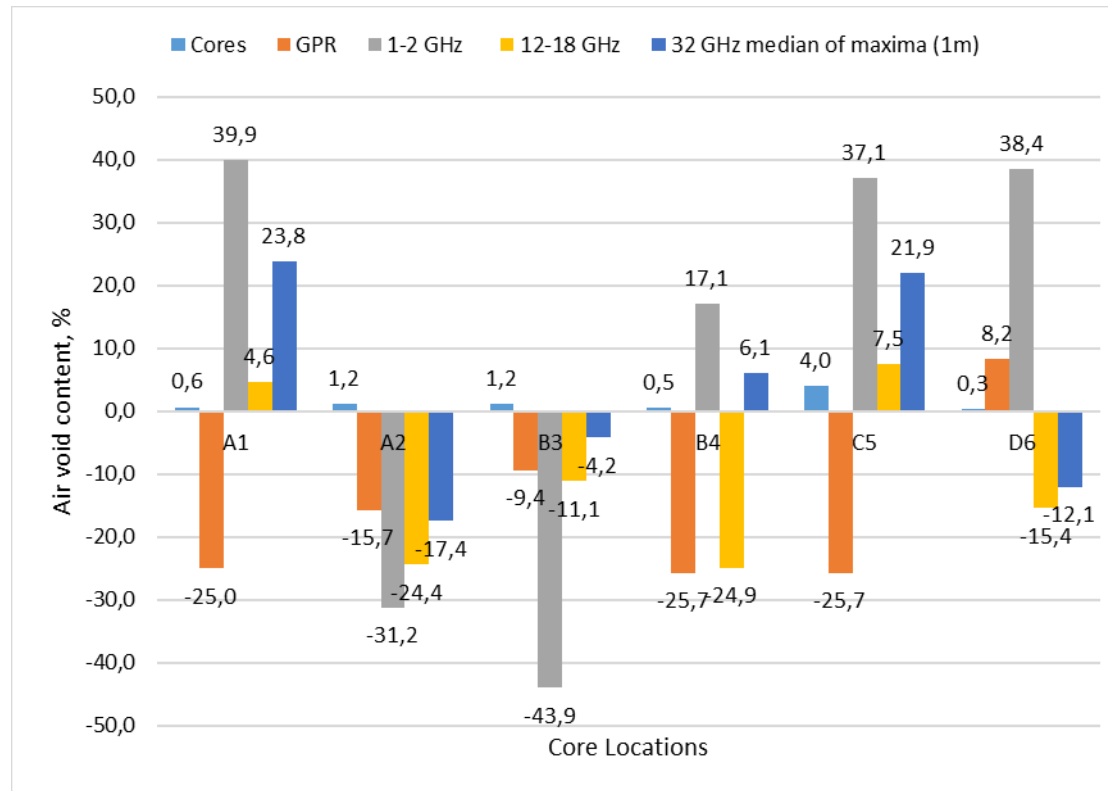




Back-calculated “stone” permittivity using CRIM model

Core Nro	Pavement Section	32 GHz median of max. (1m)	12-18 GHz	1-2 GHz	GPR
1	A	4.52	5.11	4.04	6.07
2	A	5.89	6.13	6.38	5.77
3	B	5.62	5.86	7.12	5.74
4	B	5.16	6.37	4.88	6.37
5	C	4.97	5.41	4.39	6.45
6	D	5.82	6.01	4.19	5.15
	Average	5.33	5.82	5.16	5.92
	St. Deviation	0.54	0.47	1.28	0.48

Estimated air voids using discrete modeling



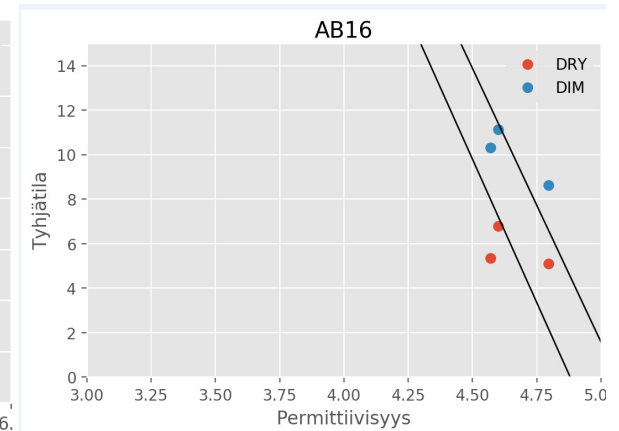
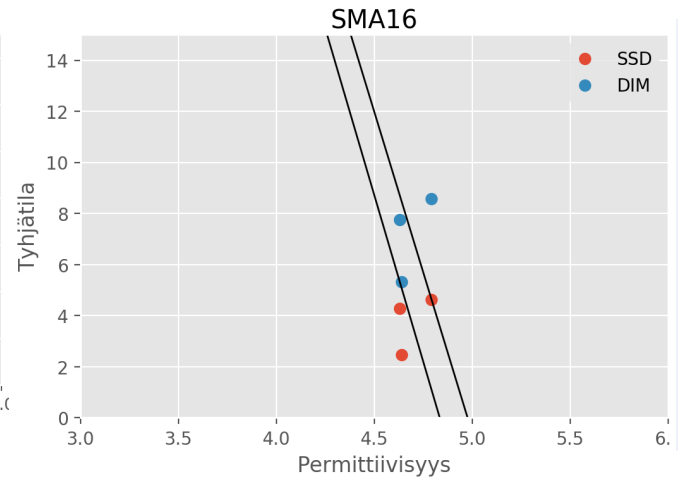
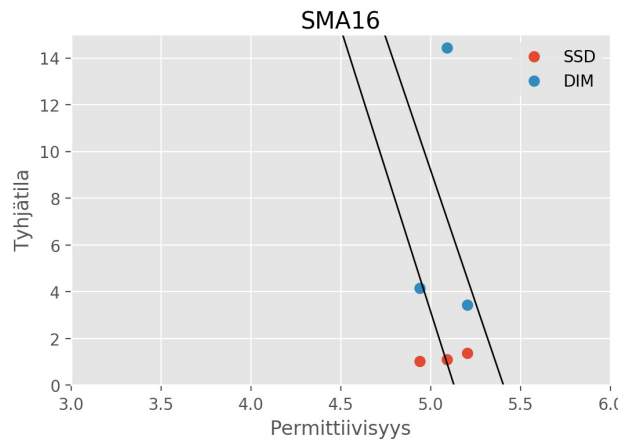
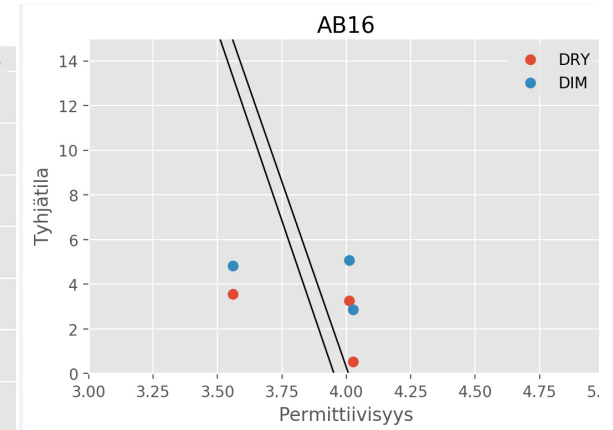
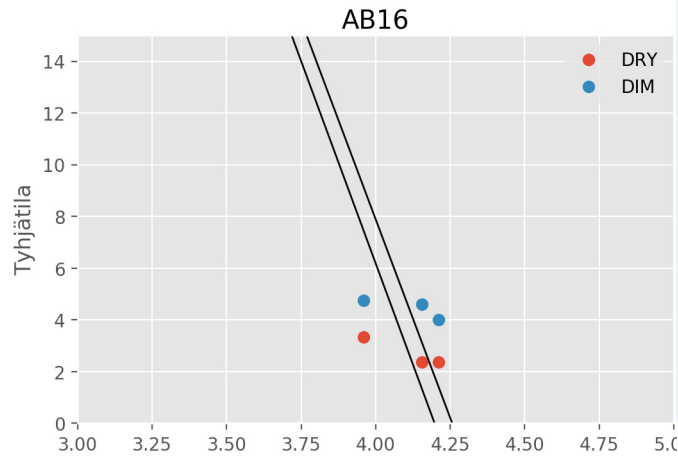


Aalto University
School of Engineering

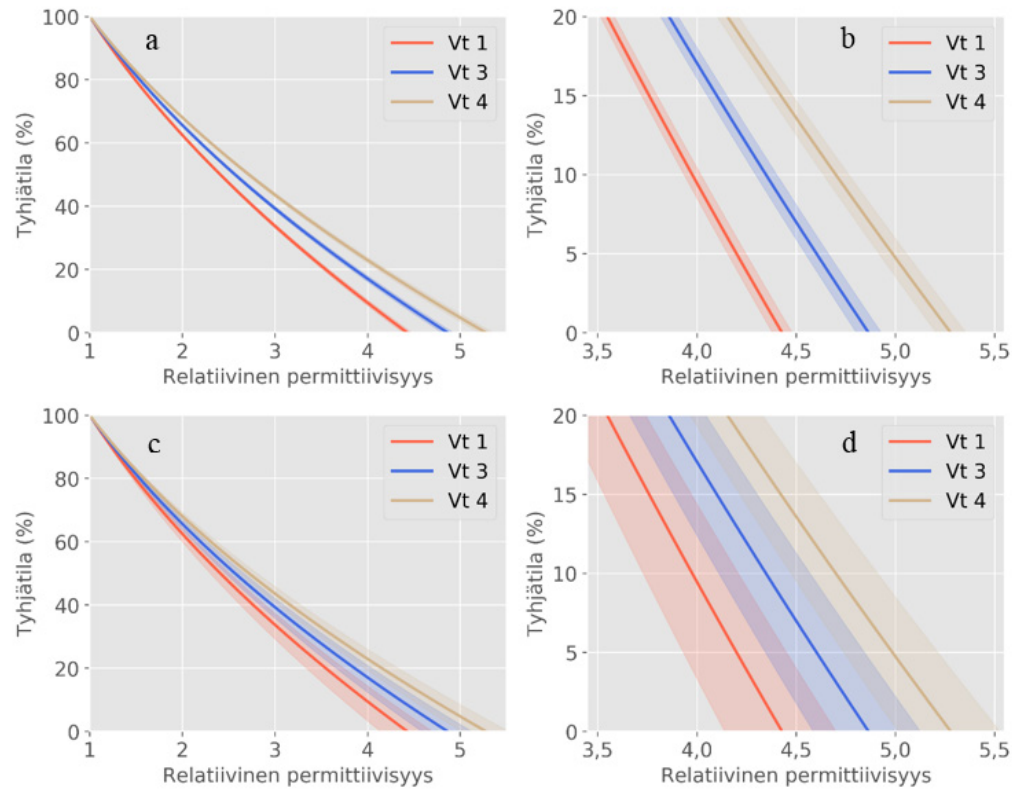
Calibration of radars



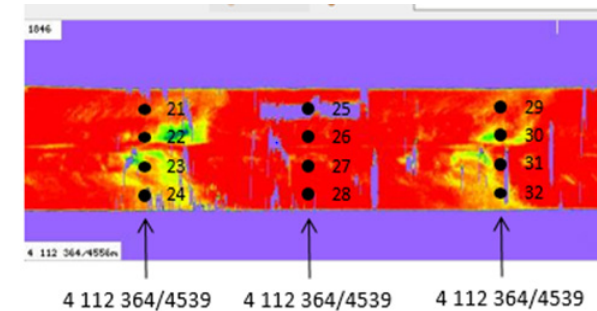
One or two cores?



Simulation of sensitivity



Mix segregation



Vt1: $\epsilon_r' = 4,5$

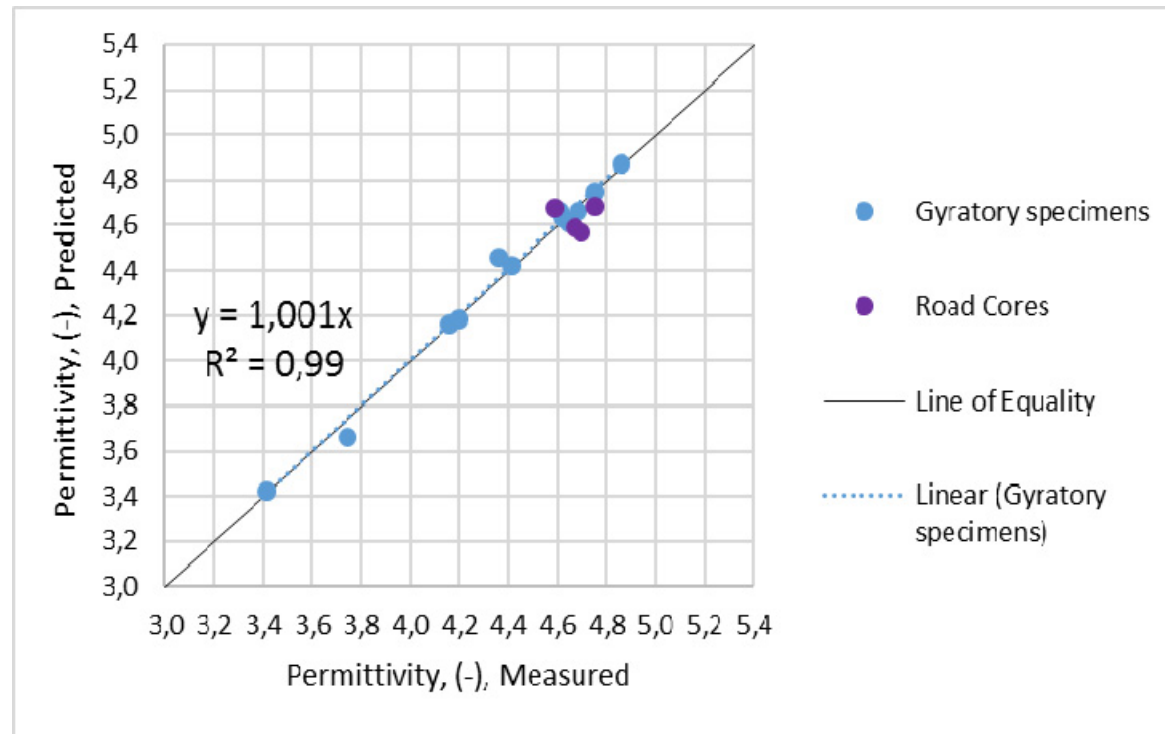
Vt3: $\epsilon_r' = 5,3$

Vt4: $\epsilon_r' = 5,8$

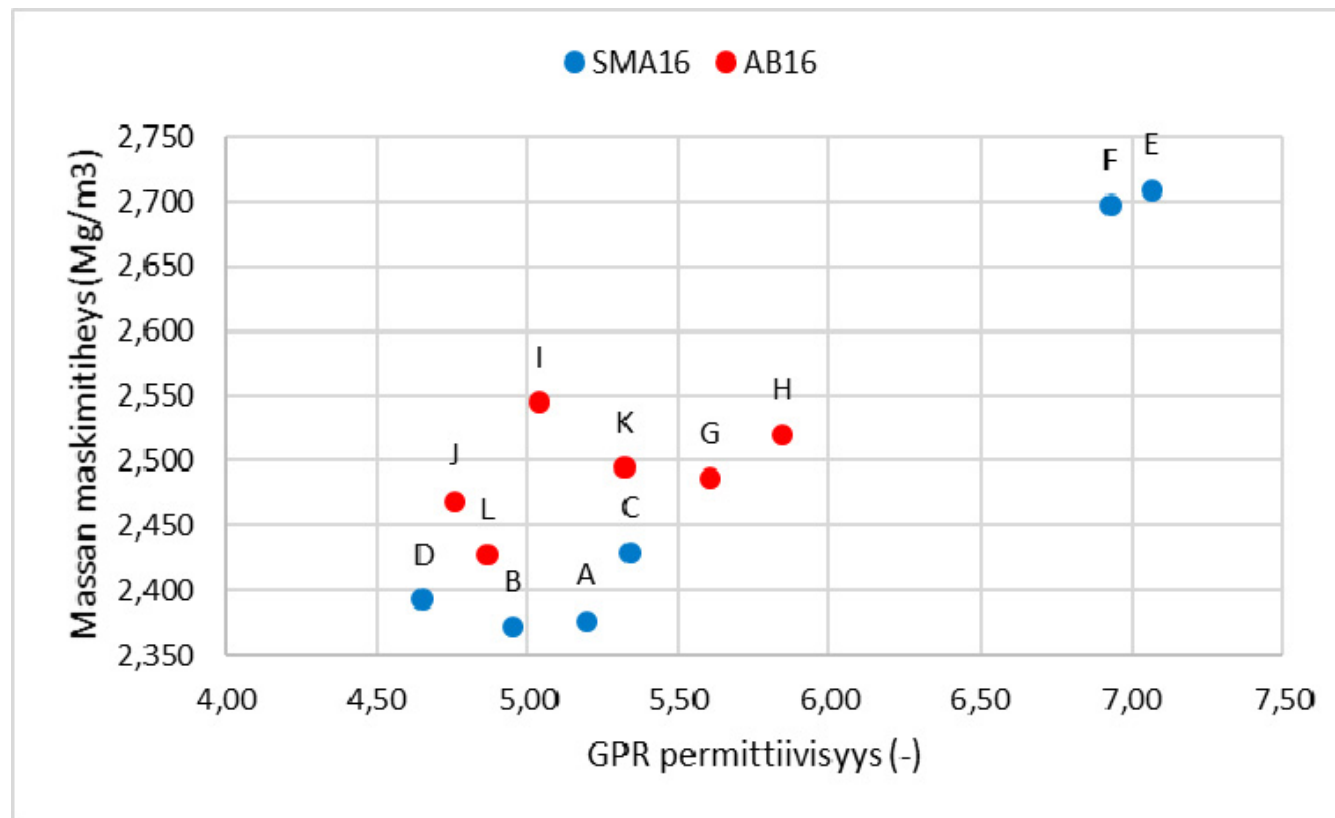
Bit% $\pm 0,5$ mass-%

**Stone variation of ϵ_r'
 $\pm 0,20$**

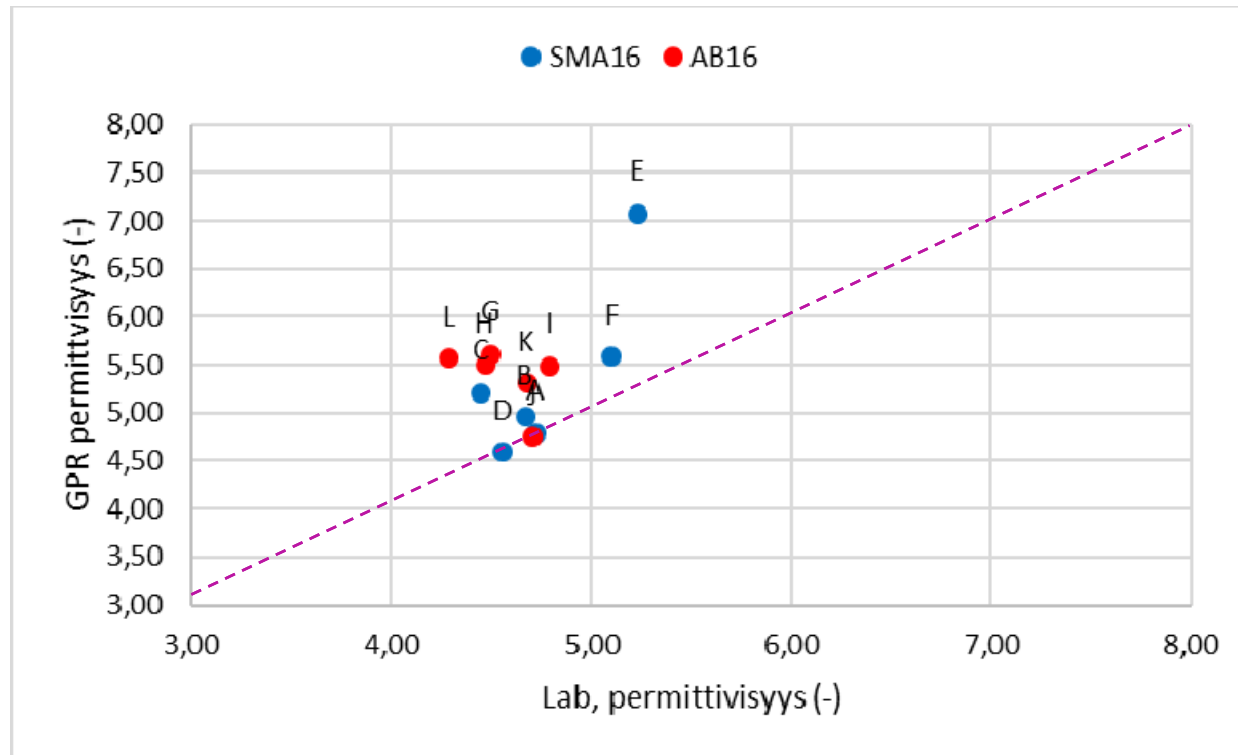
Road cores



Max density vs. permittivity from GPR



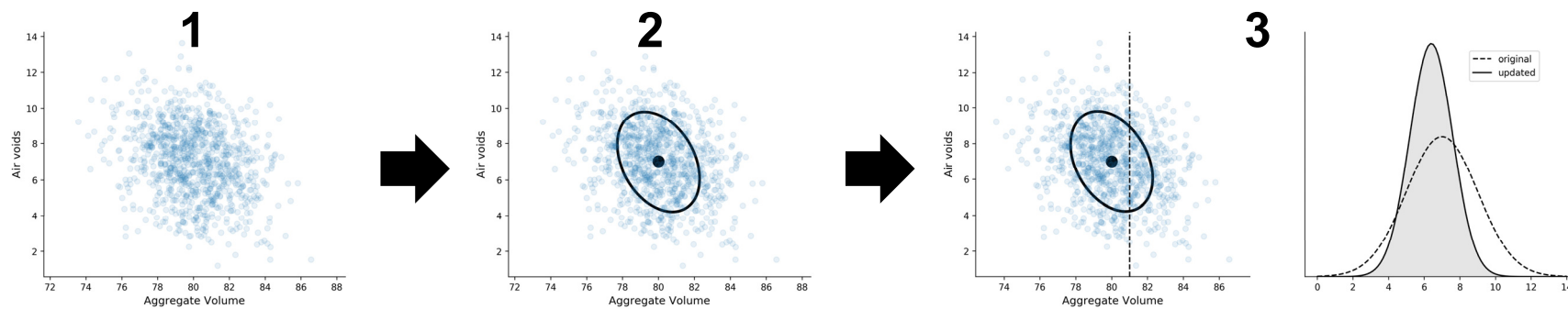
GPR vs. lab measurements



Statistical modeling

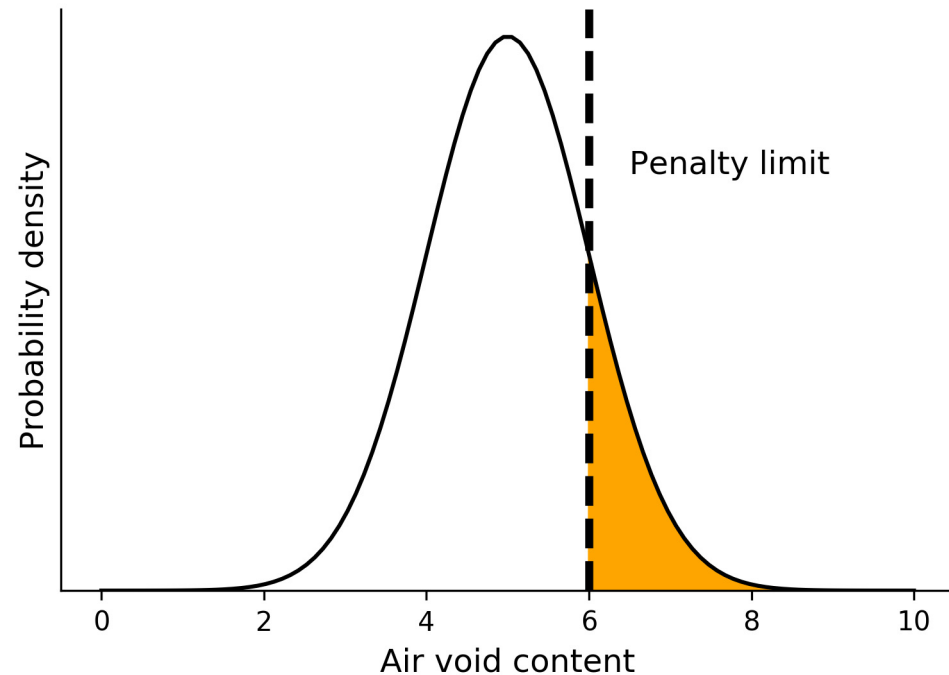
The modelling is divided to 3 steps

1. Material model
2. Multivariate Normal approximation step
3. Conditional Gaussian method



Results – Estimation of air void content

- Each measured point is modelled as a distribution (Normal) which means that with survival function we can calculate how much of the representative distance is over specified limit
- With this method a probabilistic estimate of total percent of distance over the limit can be calculated





Aalto University
School of Engineering

Thank you

Questions related to the development of radar systems:
pekka.eskelinen@aalto.fi



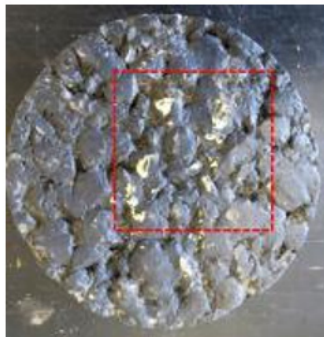
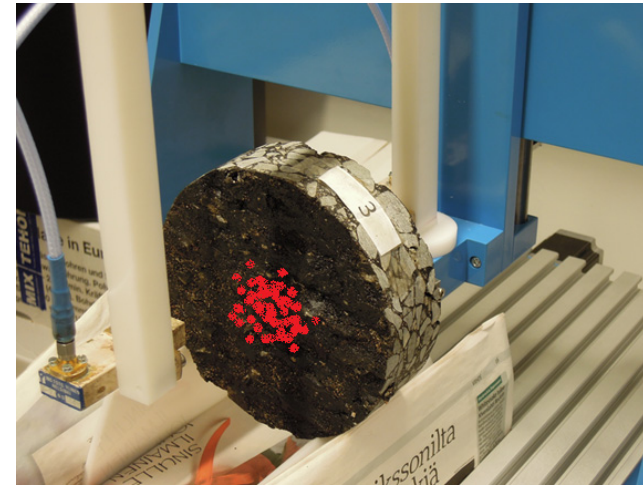
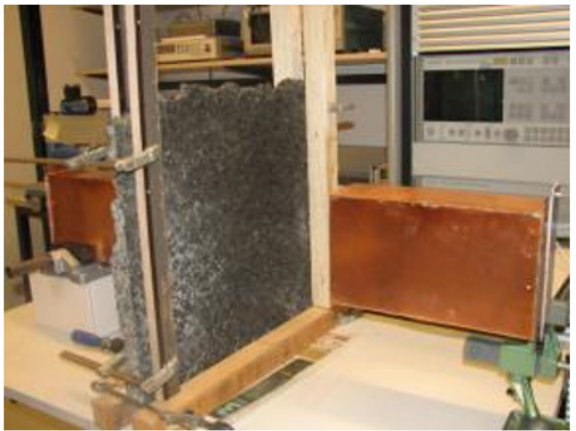
Field sampling included 37 drilled core samples and 2 slabs

GPR measurements from same locations

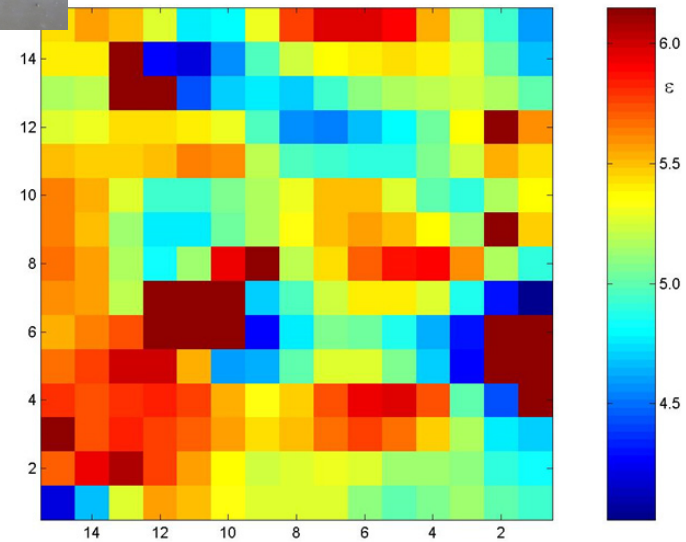
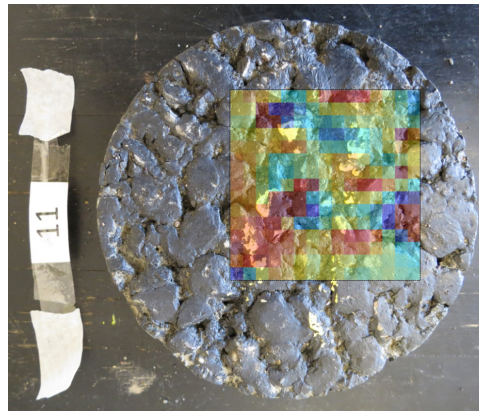
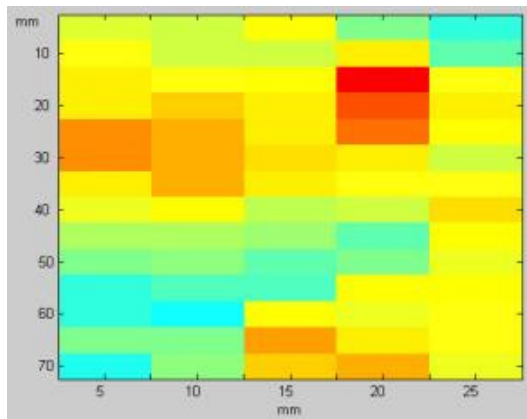
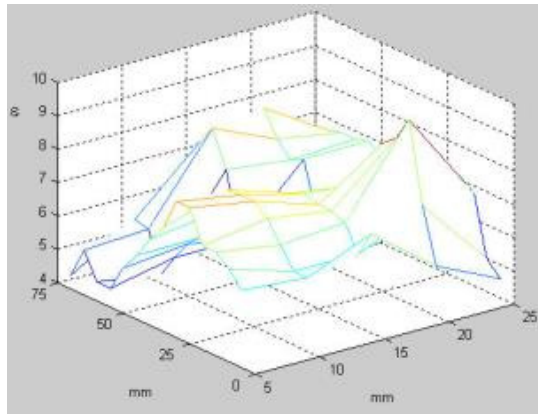




Lab trials with VNA

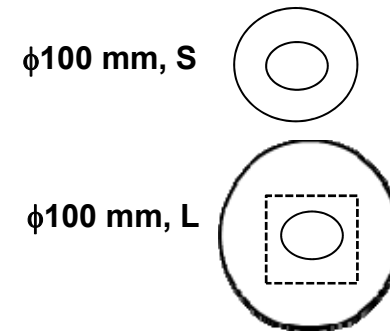
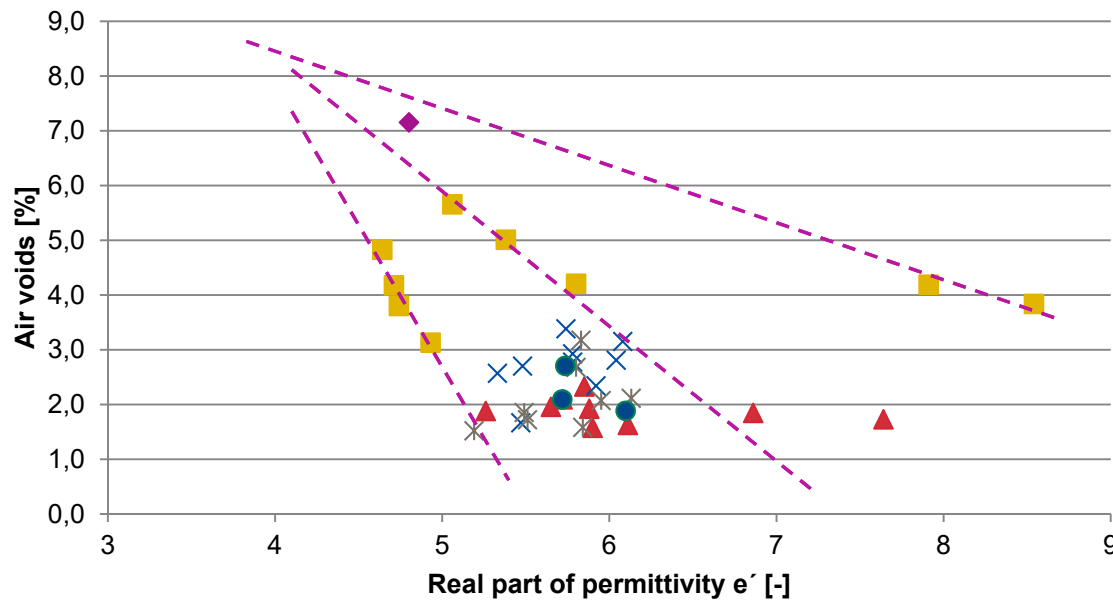


Lab trials



First results of laboratory measurements (7-17 GHz)

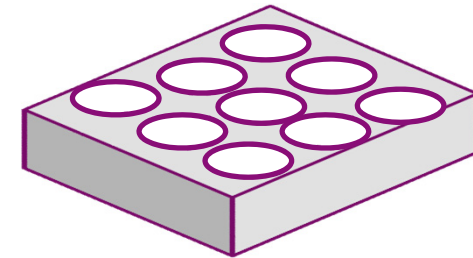
Permittivity measured 2014 with VNA



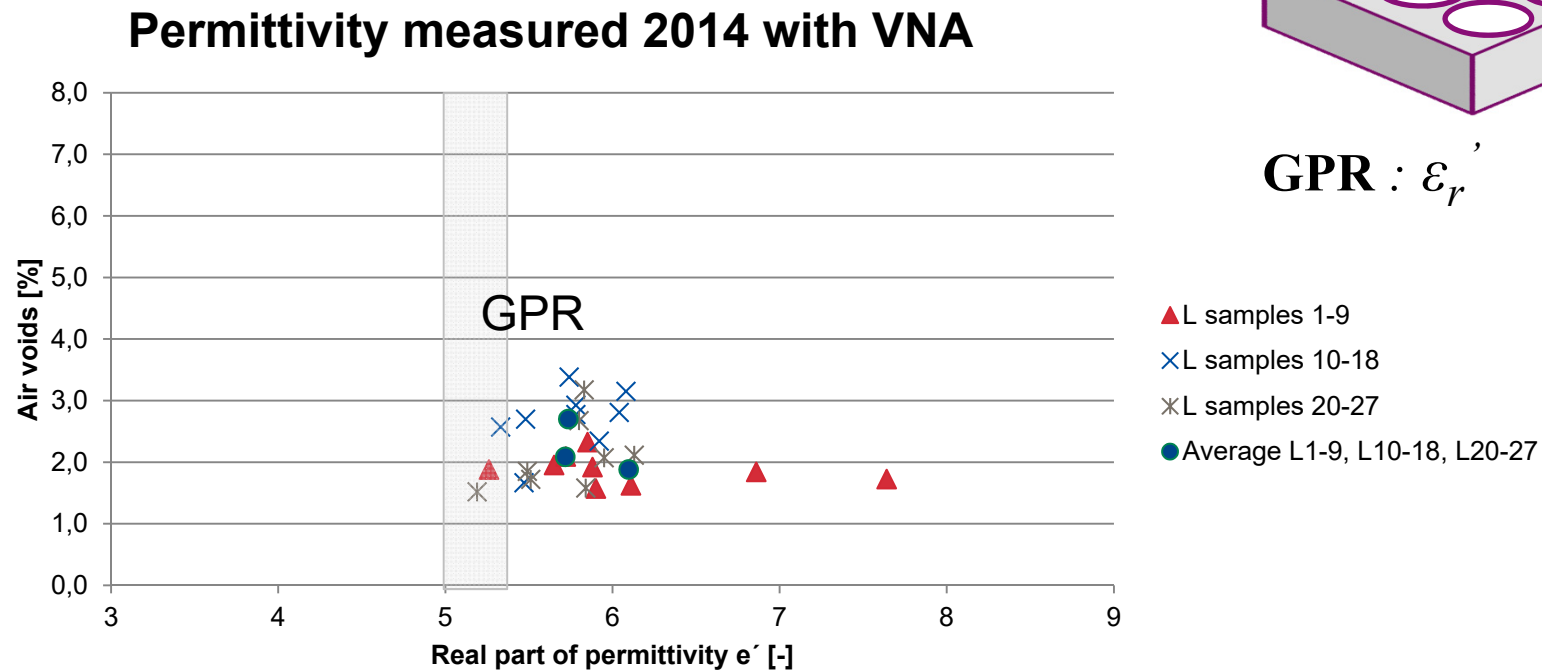
- S samples
- ◆ Slab
- ▲ L samples 1-9
- × L samples 10-18
- ✱ L samples 20-27
- Average L1-9, L10-18, L20-27

$$\sqrt{\epsilon_{eff}} = \sum_i \sqrt{\epsilon_i} V_i$$

Laboratory vs. Field Location 1



GPR : ϵ_r'



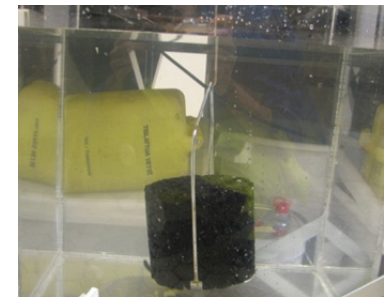
Measuring air voids in the lab

Bulk G_{mb} and maximum G_{mm} densities measured in laboratory

Air void content V_a [%]

$$V_a = \left(1 - \frac{G_{mb}}{G_{mm}} \right) \cdot 100\%$$

DRY, SSD,
PARAFILM, DIM

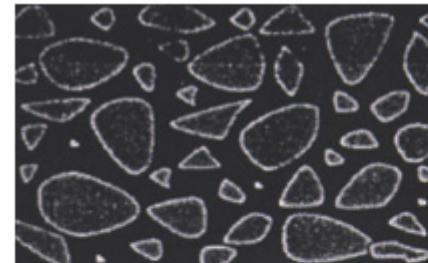


Maximum density -- no air $V_a = \left(1 - \frac{G_{mb}}{G_{mm}}\right) \cdot 100\%$

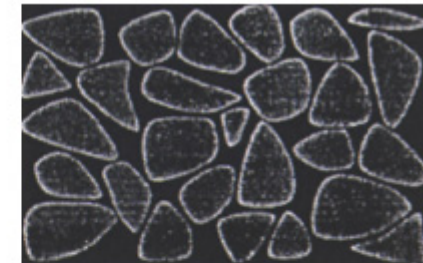


Mix types

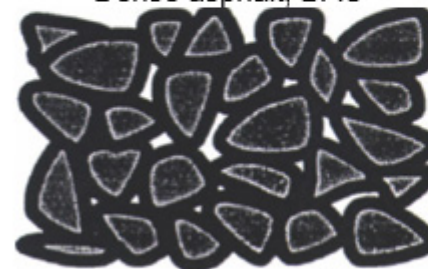
	AC	SMA	PA	MA
DRY	x	(x)	-	x
SSD	(-)	x	-	(x)
PARAF	x	x	x	x
DIM	(x)	(x)	x	(x)



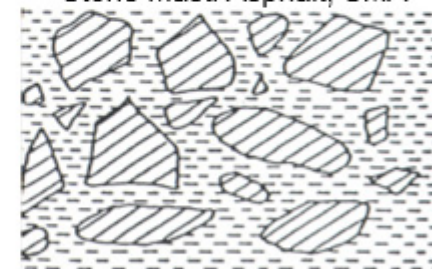
Dense asphalt, DAC



Stone Masti Asphalt, SMA



Porous asphalt, PA



Mastic asphalt, MA

Fig. 4 Asphalt mixture types and their aggregate packing arrangements.

Experiment using Gyrotory compaction

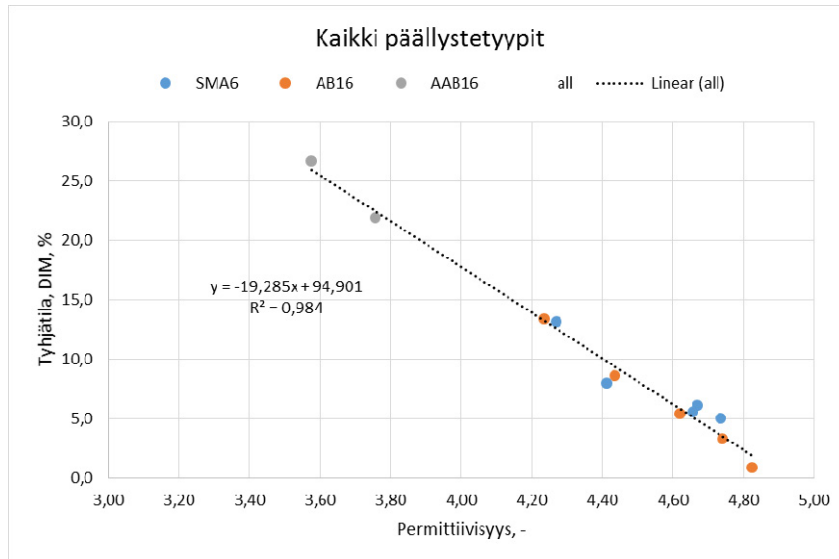
Three mixture types: AC16, SMA16, PA16

Maximum compaction: 15 to 800 gyrations

One aggregate source: granite

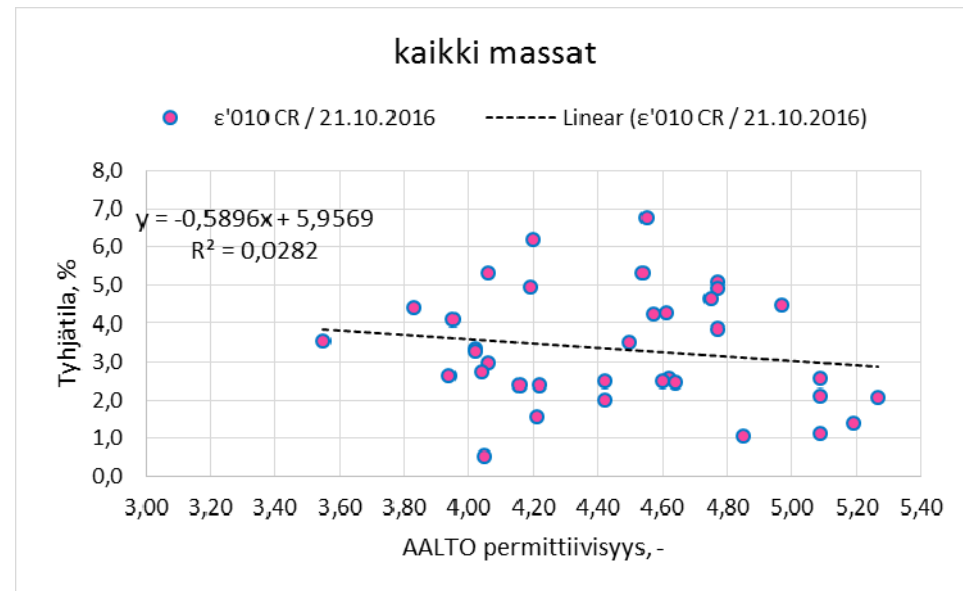
Mixture	Bit. m-%	LS m-%	Stone m-%	0-8 mm, m-%	8-16 mm, m-%	Fiber m-%
SMA16	6,0	7,5	92,5	20,5	72	0,4
AC16	5,1	2,0	98,0	65,0	33	-
PA16	4,5	0,0	100,0	22	78	-

Calibration equation?

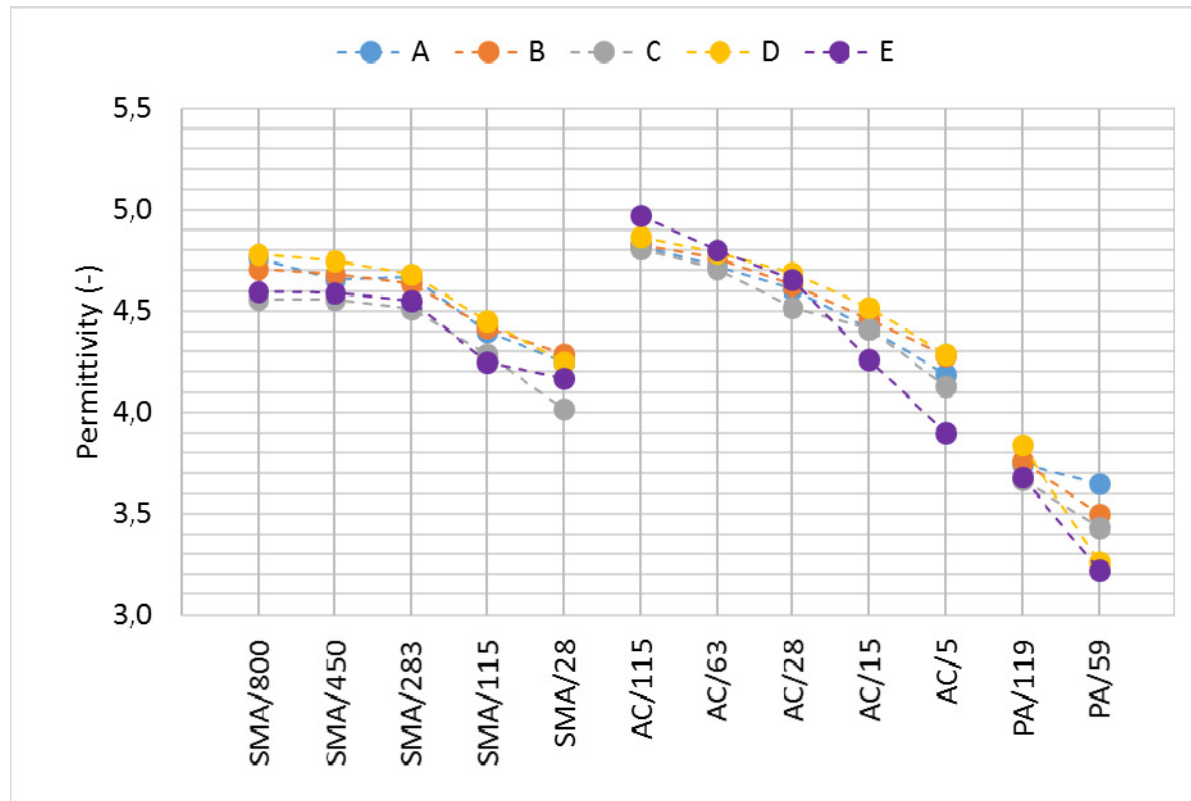


- No bitumen content variation
- No aggregate variation

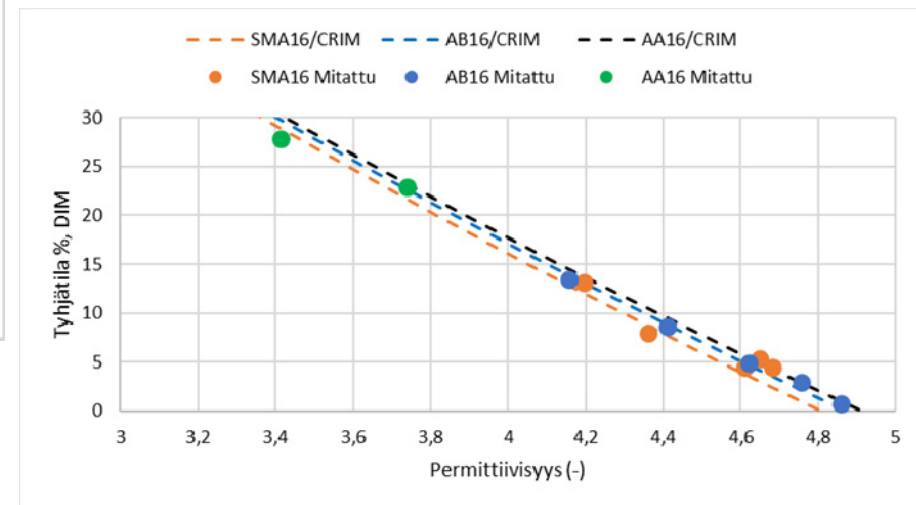
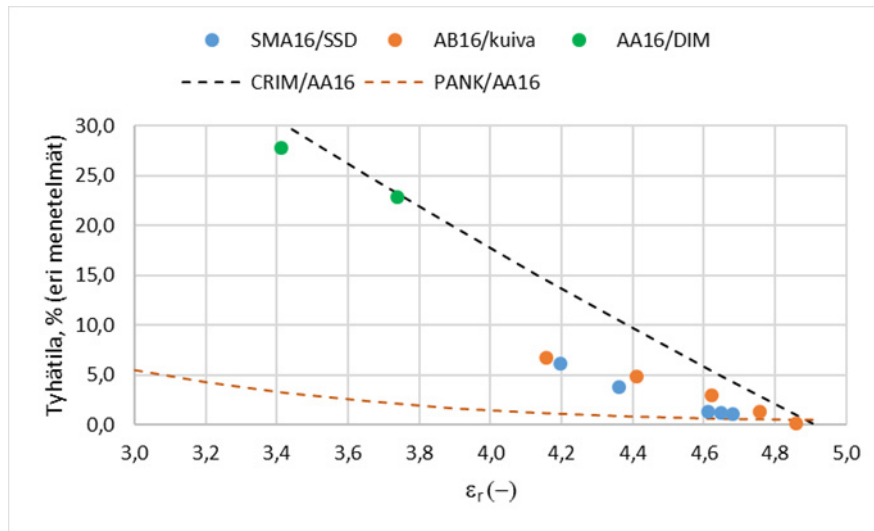
- Normal production bitumen content variation
- Normal aggregate source variation



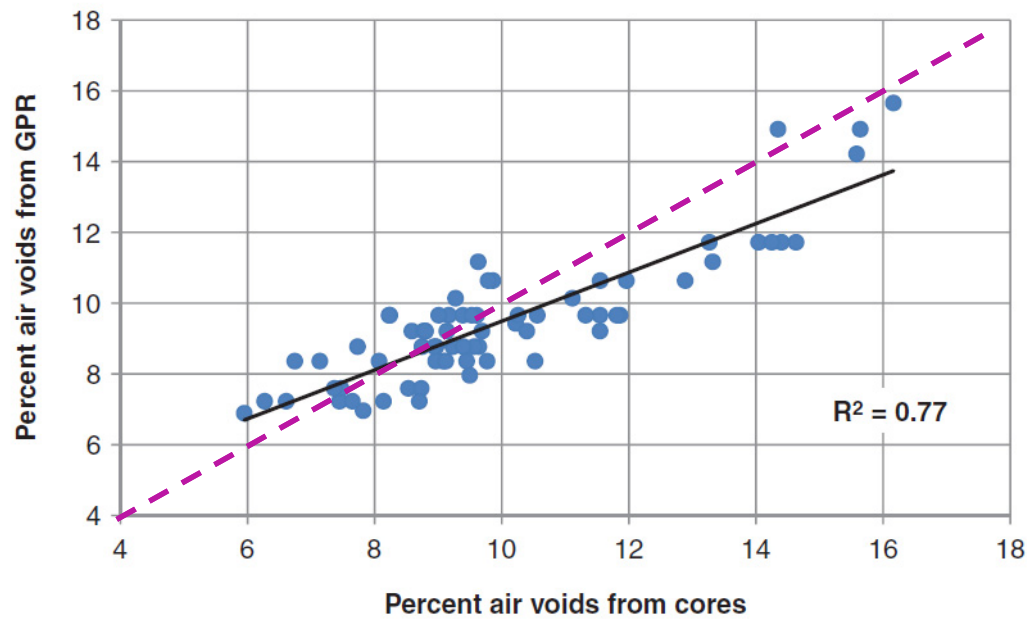
Results for permittivity



Air voids vs. permittivity



Literature



AC 9,5 mm and AC12,5 mm

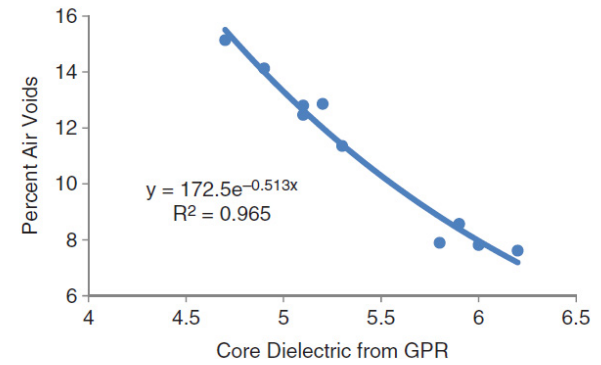
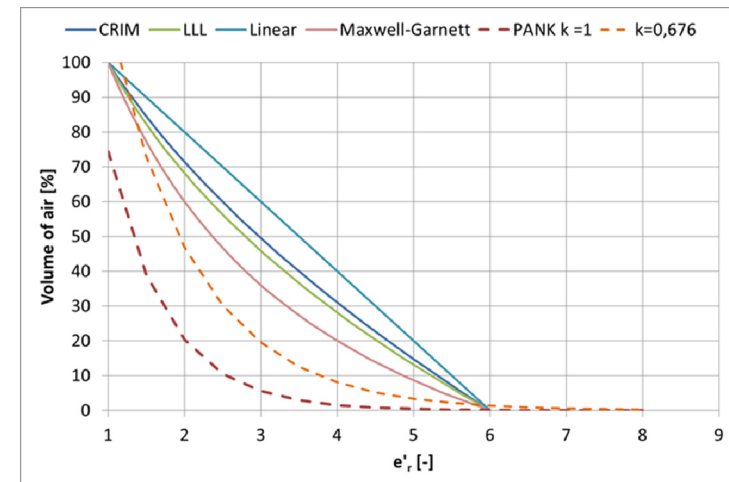
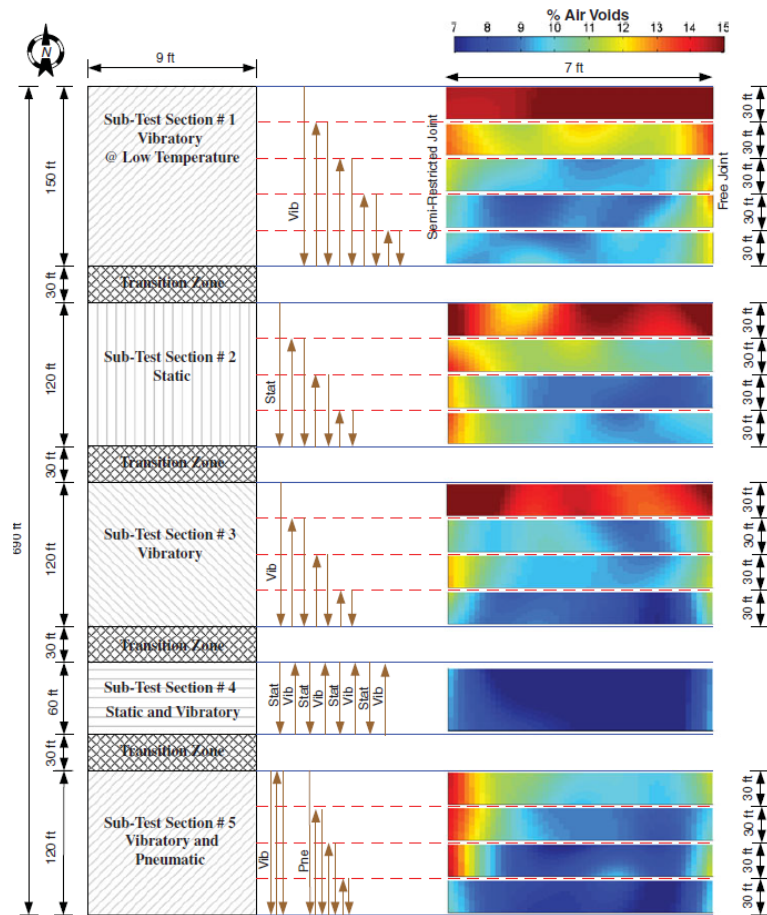


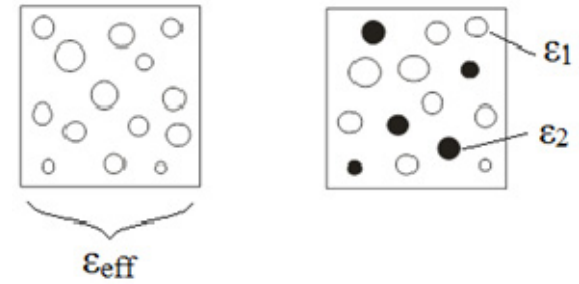
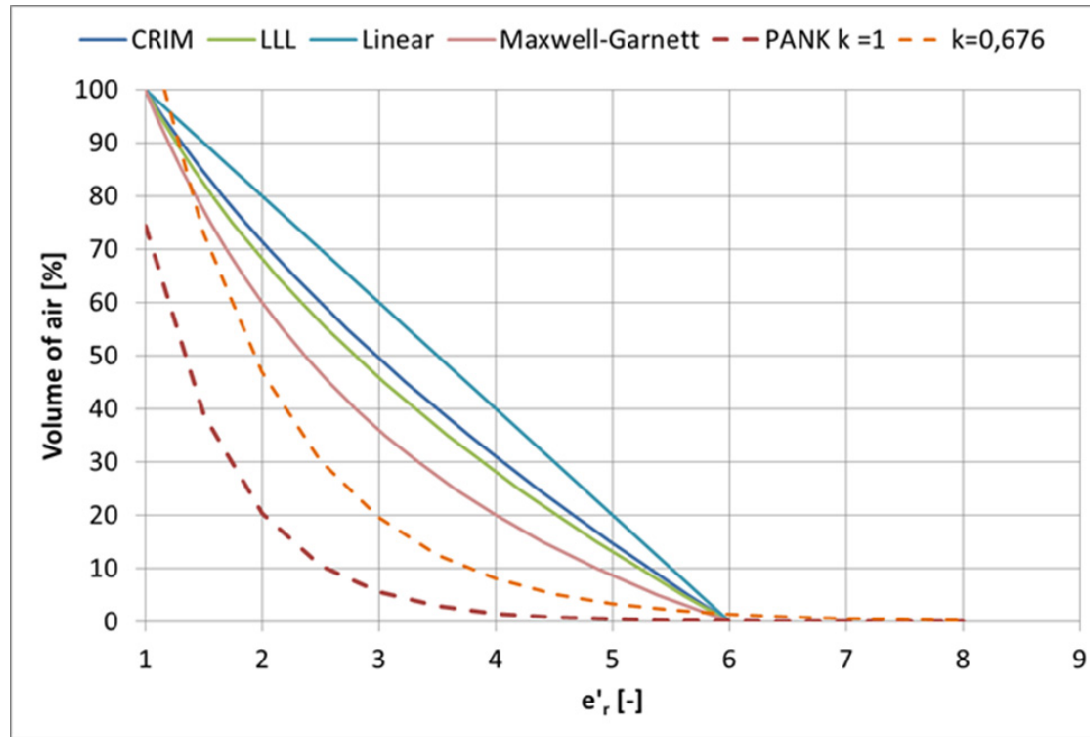
Figure 5. Correlation between dielectric constant and percent air voids of recovered cores.





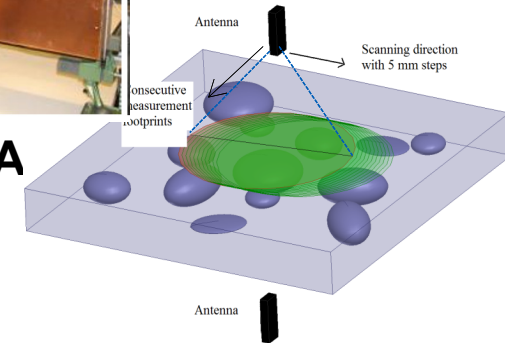
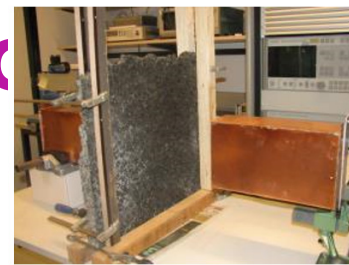
- The GPR was found to be an effective tool for assessing the compaction level in asphalt pavements.
- There was an excellent correlation between GPR air void distribution maps and the air-void maps generated from density measurements of extracted cores.
- This application of GPR is useful to obtain maps of air voids in asphalt pavements **at relatively low cost** and without causing interference to traffic.

EM mixing models

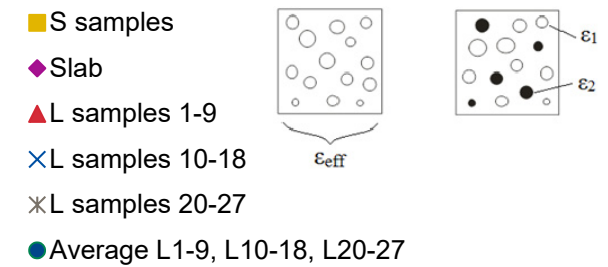
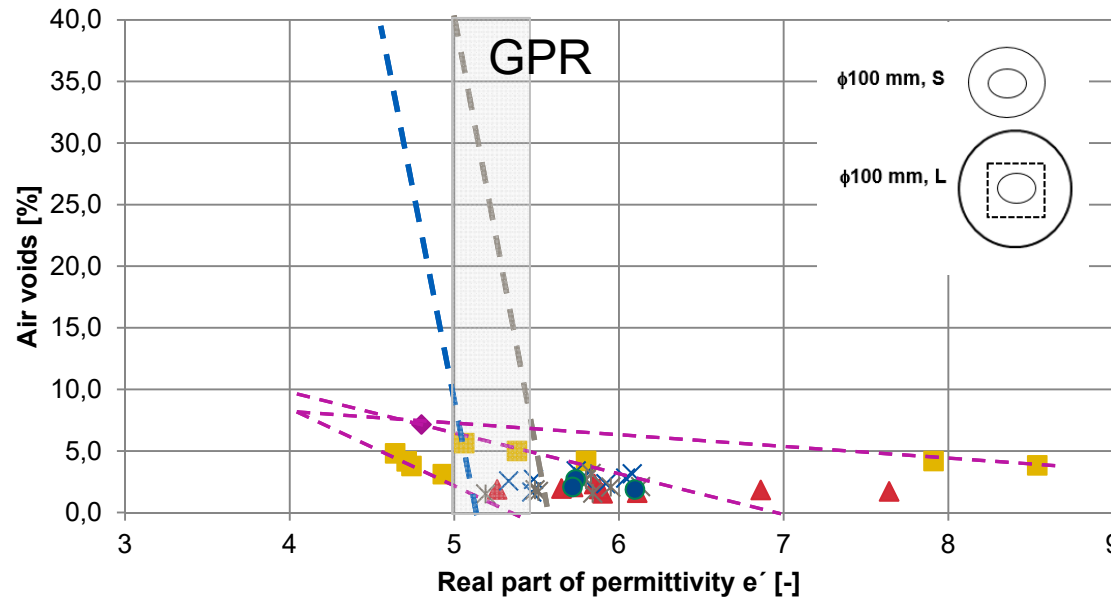


$$\epsilon'_{r,eff} = \left[\sum V_i (\epsilon'_{r,i})^\alpha \right]^{\frac{1}{\alpha}}$$

First results of laboratory measurements



Permittivity measured 2014 with VNA



$$\sqrt{\epsilon_{eff}} = \sum_i \sqrt{\epsilon_i} V_i$$